AD-A032 946 STEVENS INST OF TECH HOBOKEN N J DAVIDSON LAB F/G 20/4
ANALYTICAL INVESTIGATION OF THE QUADRATIC FREQUENCY RESPONSE FO--ETC(U)
AUG 76 J F DALZELL, C H KIM N00014-76-C-0347
UNCLASSIFIED SIT-DL-76-1878 NL

| OF |
AD
A032946

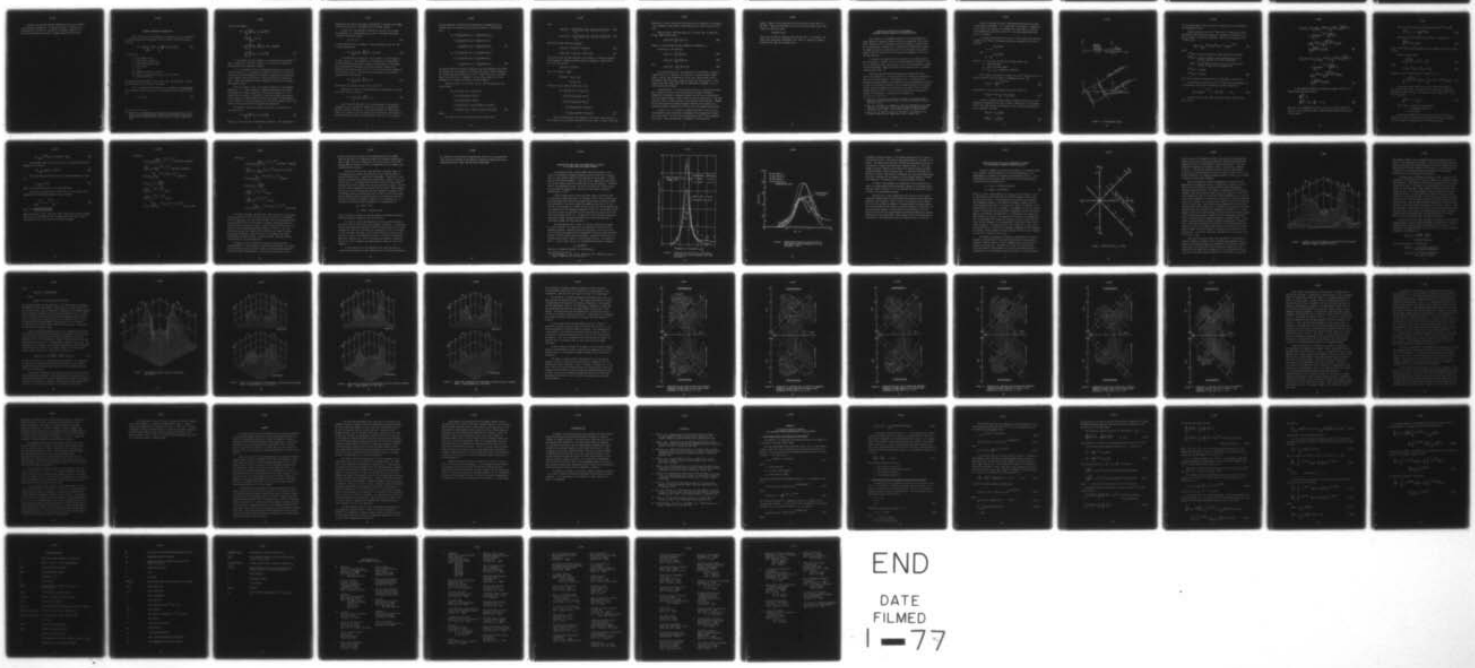

END

DATE
FILMED
1-77

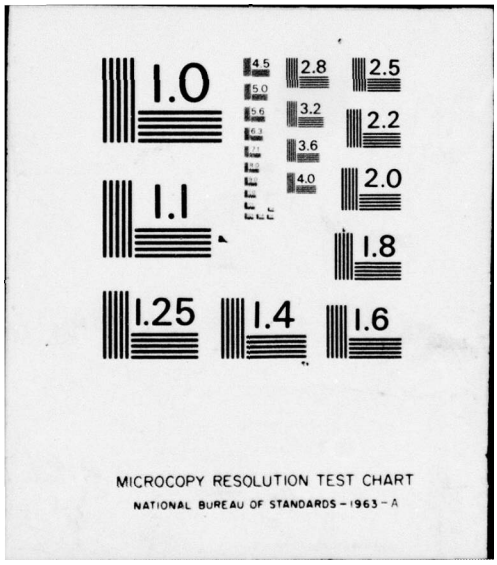
1.0
1.1
1.25
1.4
1.6
1.8
2.0
2.2
2.5
2.8
3.2
3.6
4.0
4.5
5.0
5.6
6.3
MICROCOPY RESOLUTION TEST CHART
NATIONAL BUREAU OF STANDARDS - 1963 - A

STEVENS INSTITUTE
OF TECHNOLOGY

CASTLE POINT STATION
HOBOKEN, NEW JERSEY 07030

DAVIDSON LABORATORY

Report SIT-DL-76-1878

ANALYTICAL INVESTIGATION OF THE QUADRATIC FREQUENCY RESPONSE FOR ADDED RESISTANCE

by

J.F. Dalzell and C.H. Kim

August 1976

Final Report
1 October 1975 to 30 September 1976

Prepared for
David Taylor Naval Ship Research
and Development Center (1505)
Bethesda, Maryland 20084

Office of Naval Research
800 N. Quincy Street
Arlington, Virginia 22217

UNCLASSIFIED

SECURITY CLASSIFICATION OF THIS PAGE *(When Data Entered)*

REPORT DOCUMENTATION PAGE

READ INSTRUCTIONS BEFORE COMPLETING FORM

1. REPORT NUMBER (14) SIT-DL-76-1878	2. GOVT ACCESSION NO. /
3. RECIPIENT'S CATALOG NUMBER (9)	
4. TITLE *(and Subtitle)* (6) ANALYTICAL INVESTIGATION OF THE QUADRATIC FREQUENCY RESPONSE FOR ADDED RESISTANCE.	5. TYPE OF REPORT & PERIOD COVERED FINAL Rept. 1 Oct 1975 — 30 Sept 1976
	6. PERFORMING ORG. REPORT NUMBER SIT-DL-76-1878
7. AUTHOR(s) (10) J.F. Dalzell and C.H. Kim	8. CONTRACT OR GRANT NUMBER(s) (15) N00014-76-C-0347 NEW
9. PERFORMING ORGANIZATION NAME AND ADDRESS Davidson Laboratory Stevens Institute of Technology Castle Point Station, Hoboken, NJ 07030	10. PROGRAM ELEMENT, PROJECT, TASK AREA & WORK UNIT NUMBERS SR 023 01 01
11. CONTROLLING OFFICE NAME AND ADDRESS David Taylor Naval Ship Research and Development Center Bethesda, MD 20084	(11) 12. REPORT DATE August 1976 13. NUMBER OF PAGES ii + 66 pages
14. MONITORING AGENCY NAME & ADDRESS *(if different from Controlling Office)* Office of Naval Research 800 N. Quincy Street Arlington, VA 22217 (12) 71 p.	15. SECURITY CLASS. *(of this report)* UNCLASSIFIED
	15a. DECLASSIFICATION/DOWNGRADING SCHEDULE

16. DISTRIBUTION STATEMENT *(of this Report)*

APPROVED FOR PUBLIC RELEASE; DISTRIBUTION UNLIMITED

(16) SR0230101

17. DISTRIBUTION STATEMENT *(of the abstract entered in Block 20, if different from Report)*

(17) SR0230101

D D C RECEIVED DEC 6 1976

18. SUPPLEMENTARY NOTES

Sponsored by the Naval Sea Systems Command, General Hydromechanics Research Program--administered by the David Taylor Naval Ship Research and Development Center, Code 1505, Bethesda, MD 20084

19. KEY WORDS *(Continue on reverse side if necessary and identify by block number)*

GHR Program; Added Resistance, Quadratic Response, Non-Linear Response

20. ABSTRACT *(Continue on reverse side if necessary and identify by block number)*

The objective of the present work was to extend existing hydrodynamic theory for ship resistance added by waves to include time dependent fluctuations, so that the so-called "quadratic frequency response function" for added resistance could be computed and compared with previously obtained experimental estimates. The concept of a quadratic frequency response function follows from the (non-physical) theory for the general functional polynomial input-output model which was utilized in the previous experimental

next page →

DD FORM 1 JAN 73 1473 EDITION OF 1 NOV 65 IS OBSOLETE S/N 0102-014-6601

UNCLASSIFIED 104750

SECURITY CLASSIFICATION OF THIS PAGE *(When Data Entered)*

20. work. It was hoped that the present work, by providing a physical model, would either lend credibility to the previous work or expose its shortcomings. In the event, the present work appears to have accomplished both. Analytical and experimental estimates of the quadratic frequency response function are in good qualitative agreement, and in fair quantitative agreement. Most of those experimental estimates which appeared in the previous work to be of at least slightly dubious statistical merit have been discredited. Since it was these marginal experimental estimates which gave rise to the speculation that the quadratic frequency response function was inordinately complicated, the present work indicates that the function is merely moderately complicated. There seems reasonable evidence that it is feasible to make hydrodynamic estimates of the quadratic frequency response function required for prediction of non-linear fluctuations of resistance in random seas.

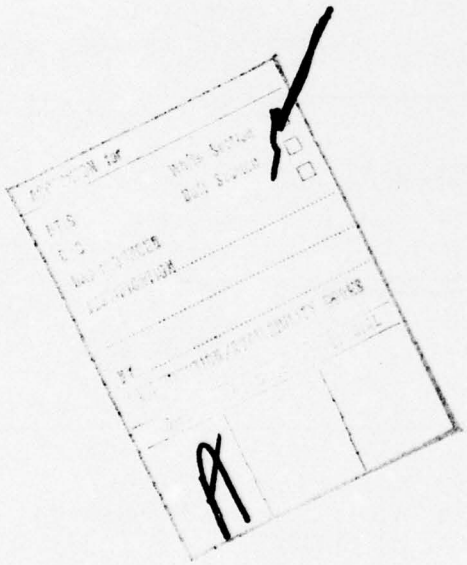

STEVENS INSTITUTE OF TECHNOLOGY
DAVIDSON LABORATORY
CASTLE POINT STATION
HOBOKEN, NEW JERSEY

REPORT SIT-DL-76-1878

August 1976

ANALYTICAL INVESTIGATION OF THE QUADRATIC FREQUENCY RESPONSE FOR ADDED RESISTANCE

by

J.F. Dalzell and C.H. Kim

This research was carried out under the
Naval Sea Systems Command
General Hydromechanics Research Program
SR 023-01-01 administered by the
David Taylor Naval Ship Research and Development Center
under Contract N00014-76-C-0347

(DL Project 4366/176)

Approved

John P. Breslin
Director

CONTENTS

INTRODUCTION

The present work follows from that summarized in Ref. 1.* The objective of the previous work was to demonstrate by means of analyses of experimental data that a functional polynomial input-output model for added resistance in waves was a reasonable engineering approximation. The results obtained indicated that this is so. It was demonstrated that it is possible to identify a quadratic frequency response function for added resistance from experiments in both regular and irregular waves; and that, given the frequency domain response, it is possible to synthesize in the time domain at least the low frequency nonlinear resistance components.

The general approach in the cited work was to accept a particular input-output model as an hypothesis and to attempt its validation by analyses of data obtained in towing tank tests in irregular waves. The idea that a "quadratic frequency response function" for added resistance exists and is meaningful followed from the hypothesized input-output model. This idea was considerably strengthened by utilizing the first three complete cross-bi-spectral analyses of experimental data to identify the non-linear responses resulting from the interactions of input frequencies. Empirical collapse of estimates was obtained for some of the prominent features of the quadratic frequency response function over a wide range of sea severity. However the work also indicated that the quadratic frequency response function for added resistance is quite complicated -- more so in fact than could be reliably determined from the available experimental data.

Thus in the cited work the identification of the complete quadratic response function was necessarily confined to what could be inferred from existing experimental measurements, and from the general (non physical)

---

*1. Dalzell, J.F., "Application of the Functional Polynomial Model to the Ship Added Resistance Problem," Paper presented at the Eleventh Symposium on Naval Hydrodynamics, London, March 1976.

theory. The weakest part of the argument that a meaningful added resistance quadratic response function exists was that there existed no confirming information about the general nature and behavior of the complete function. All previous theoretical and experimental investigations had involved the "mean added resistance operator" which is only the value of the quadratic frequency response function along a very special line in the bi-frequency plane. According to the experimental results there appeared to be some important input frequency interaction response at combinations of frequencies not resolved by experiment but possible in full scale.

It was clear that even an approximate extension of existing hydrodynamic theory for added resistance to include the general response case would provide considerable insight into the nature of resistance fluctuations in random seas, and, by providing a physical model, either lend credibility to the previous work or help expose its short-comings. This was the general objective of the present work. The specific work carried out involved an extension of existing hydromechanic theory, computations of quadratic frequency response according to this extension for one of the experimental cases of the previous work, and a comparison of the results with experiment.

THE INPUT-OUTPUT MODEL

A few definitions and relations pertaining to the general input-output model are needed in the present work. These will be given here for convenience, though they may be found in Ref. 1, or (in generally greater detail) in the series of references[2,3,4,5*] which form the source material for Ref. 1.

The general input-output model is a time domain model and is written as:

$$D_w(t) = \int g_1(t_1)\eta(t-t_1)dt_1 + \iint g_2(t_1,t_2)\eta(t-t_1)\eta(t-t_2)dt_1\,dt_2 \qquad (1)$$

(Omission of limits on the integrals signifies limits of $\pm\infty$.)

In Eq. (1): $D_w(t)$ is the resistance added by waves (the output)

$\eta(t)$ is a suitably chosen wave elevation (a zero mean input)

$g_1(t)$ is a linear impulse response

$g_2(t_1,t_2)$ is a second degree kernel analogous to an impulse response

---

*2. Dalzell, J.F., "Application of Cross-Bi-Spectral Analysis to Ship Resistance in Waves," SIT-DL-72-1606, AD749102, Davidson Laboratory, Stevens Institute of Technology, May 1972.

3. Dalzell, J.F., "Some Additional Studies of the Application of Cross-Bi-Spectral Analysis to Ship Resistance in Waves," SIT-DL-72-1641, AD757363, Davidson Laboratory, Stevens Institute of Technology, December 1972.

4. Dalzell, J.F., "Cross-BiSpectral Analysis: Application to Ship Resistance in Waves," Journal of Ship Research, Vol. 18, No. 1, March 1974, pp 62-72.

5. Dalzell, J.F., "The Applicability of the Functional Polynomial Input-Output Model to Ship Resistance in Waves," SIT-DL-75-1794, Davidson Laboratory, Stevens Institute of Technology, January 1975.

With respect to application to added resistance, the ship is assumed to be proceeding at constant forward velocity in a wave system (the input) which is defined as the wave elevation at a point stationary with respect to the mean position of the ship; that is, Eq. (1) is an encounter domain model. The second degree kernel is assumed to be symmetric in its arguments, and both kernels are assumed smooth and absolutely integrable.

The first term in Eq. (1) is the ordinary linear convolution of a linear impulse response function $g_1(t_1)$ with $\eta(t)$. The second term is a double convolution, and the second degree kernel $g_2(t_1,t_2)$ might be called a quadratic impulse response. According to basic assumptions, the two impulse responses are related to the linear and quadratic frequency response functions through the Fourier transform. These two sets of transform pairs may be defined as follows:

$$g_1(\tau) = \frac{1}{2\pi}\int e^{+i\omega\tau}\, G_1(\omega)\, d\omega$$

$$G_1(\omega) = \int e^{-i\omega\tau}\, g_1(\tau)\, d\tau \qquad (2)$$

$$g_2(\tau_1,\tau_2) = \frac{1}{(2\pi)^2}\iint \mathrm{Exp}[+i\omega_1\tau_1 + i\omega_2\tau_2]\, G_2(\omega_1,\omega_2)\, d\omega_1\, d\omega_2$$

$$G_2(\omega_1,\omega_2) = \iint \mathrm{Exp}[-i\omega_1\tau_1 - i\omega_2\tau_2]\, g_2(\tau_1,\tau_2)\, d\tau_1\, d\tau_2 \qquad (3)$$

The linear frequency response function, $G_1(\omega)$, defined by Eq. (2) is absolutely conventional. The quadratic frequency response function, $G_2(\omega_1,\omega_2)$ is defined in a <u>bi-frequency</u> plane. Because the kernel $g_2(\tau_1,\tau_2)$ is assumed to be symmetrical in its arguments:

$$g_2(\tau_1,\tau_2) = g_2(\tau_2,\tau_1) \qquad (4)$$

and thus:

$$G_2(\omega_1,\omega_2) = G_2(\omega_2,\omega_1) \qquad (5)$$

$$G_2^*(\omega_1,\omega_2) = G_2(-\omega_1,-\omega_2)$$

$$= G_2(-\omega_2,-\omega_1) \qquad (6)$$

(The asterisk denotes the complex conjugate.)

Figure 1 summarizes the results of applying Eq.s (5) and (6) in the bi-frequency plane for the eight possible coordinate positions of two frequencies whose absolute values are a and b. Equation (5) results in a line of symmetry along the line $\omega_2=\omega_1$. Equation (6) results in a line of symmetry of the real part of $G_2(\omega_1,\omega_2)$ defined by $\omega_2=-\omega_1$ (and it may be noted that along this line the imaginary part of the function is zero). These two lines and the ω_1,ω_2 axes divide the bi-frequency plane into octants, of which the two on either side of the positive ω_1 axis may be arbitrarily chosen for reference. The equalities shown in Figure 1 in the remaining six octants are arrived at by applying Eqs. (5) and/or (6). The assumptions of symmetry of the second degree kernel result, with Eq. (3), in a complete definition of $G_2(\omega_1,\omega_2)$ if the functions are defined in any pair of octants including a semi-axis of either frequency. Thus without loss in generality interpretation of the quadratic frequency response needs only to involve the octants on either side of the positive ω_1 axis. In these octants ω_1 is positive and $|\omega_1| \geq |\omega_2|$.

The interpretation of the quadratic frequency response function is less direct than for the linear case, but can be approached in a similar manner. If in the linear case the system is considered to be excited by

$$\eta(t) = a\cos\omega t$$

the output may then be written:

$$\mathrm{Re}\{aG_1(\omega)\,\mathrm{Exp}(i\omega t)\}$$

and $G_1(\omega)$ is interpreted in terms of normalized amplitude and phase of response.

To interpret the quadratic frequency response, <u>dual</u> harmonic excitation is necessary. Accordingly, it may be assumed that:

$$\eta(t) = a_1\cos\omega_1 t + a_2\cos\omega_2 t \qquad (7)$$

In accordance with the previous discussion of symmetry, both frequencies (ω_1,ω_2) are considered positive and $|\omega_1| \geq |\omega_2|$. The basic model, Eq. (1) is good for any zero-mean excitation. Accordingly, Eq. (7) may be substituted directly in Eq. (1). After some algebra the final result for the

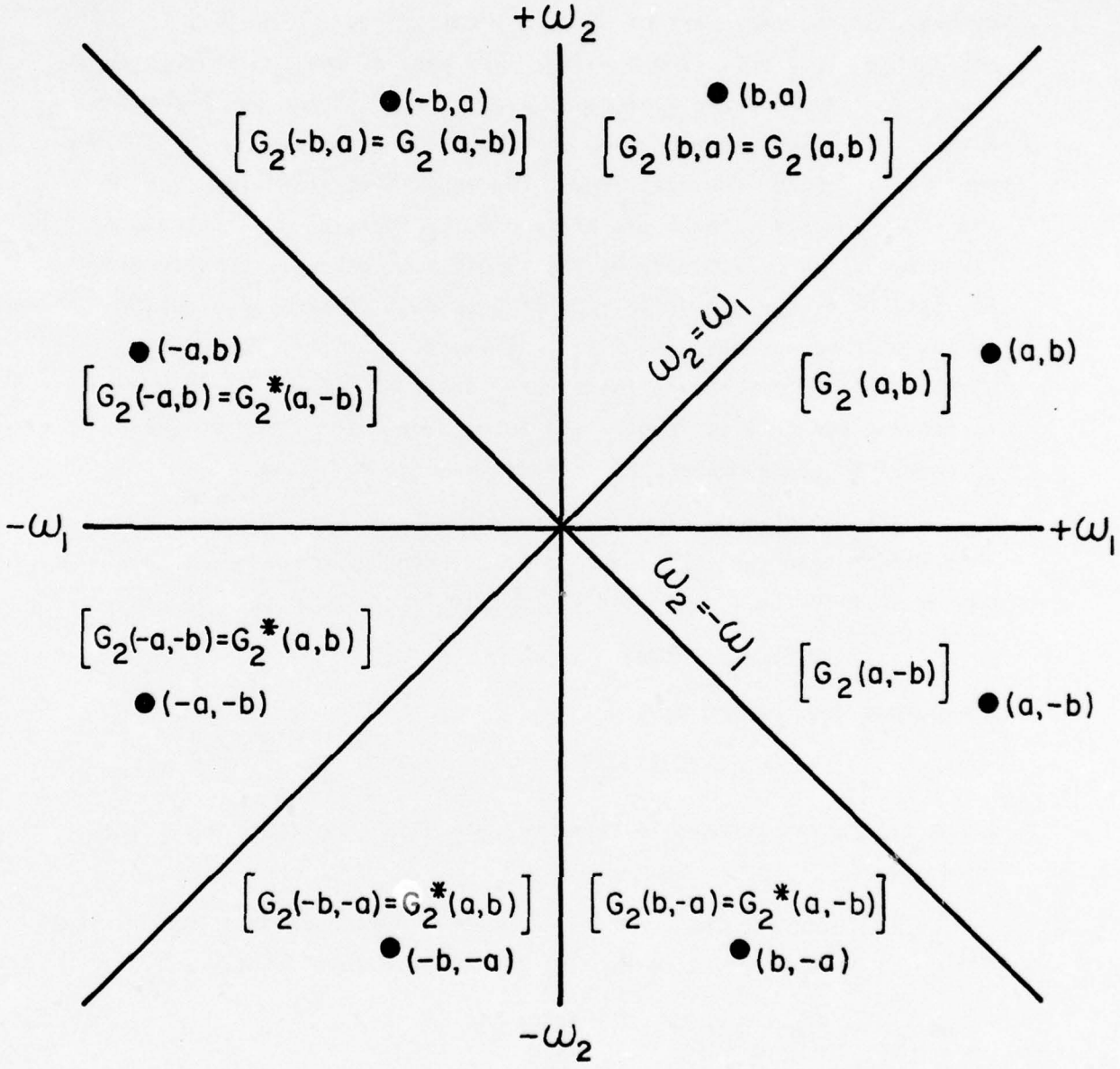

FIGURE 1 SYMMETRY OF THE QUADRATIC FREQUENCY RESPONSE FUNCTION

response to dual harmonic excitation may be written as follows:

$$
\begin{aligned}
D_2 = {} & \mathrm{Re}\{a_1 G_1(\omega_1)\,\mathrm{Exp}(i\omega_1 t) + a_2 G_1(\omega_2)\,\mathrm{Exp}(i\omega_2 t)\} \\
& + \frac{1}{2}\{a_1^2 G_2(\omega_1,-\omega_1) + a_2^2 G_2(\omega_2,-\omega_2)\} \\
& + \frac{1}{2}\,\mathrm{Re}\{a_1^2 G_2(\omega_1,\omega_1)\,\mathrm{Exp}(i2\omega_1 t)\} \\
& + \frac{1}{2}\,\mathrm{Re}\{a_2^2 G_2(\omega_2,\omega_2)\,\mathrm{Exp}(i2\omega_2 t)\} \\
& + \mathrm{Re}\{a_1 a_2 G_2(\omega_1,\omega_2)\,\mathrm{Exp}[i(\omega_1+\omega_2)t]\} \\
& + \mathrm{Re}\{a_1 a_2 G_2(\omega_1,-\omega_2)\,\mathrm{Exp}[i(\omega_1-\omega_2)t]\} \qquad (8)
\end{aligned}
$$

This result shows that the response of the quadratic system, Eq. (1), to dual excitation contains, in general, a shift in the mean and components of six different frequencies [ω_1, ω_2, $2\omega_1$, $2\omega_2$, $(\omega_1+\omega_2)$, and $(\omega_1-\omega_2)$]. The first two terms of the result are the superposition of the linear responses at the excitation frequencies. The third and fourth terms of Eq. (8) represent a shift in the mean. These terms allow the identification of the mean added resistance operator as the value of $G_2(\omega_1,\omega_2)$ along the line $\omega_2=-\omega_1$ (or $G_2(\omega_1,-\omega_1)$). The fifth and sixth terms are the second harmonic components $(2\omega_1, 2\omega_2)$. Similarly, these terms allow the identification of second harmonic response with the values of $G_2(\omega_1,\omega_2)$ along the line $\omega_2=\omega_1$ (or $G_2(\omega_1,\omega_1)$).

The seventh and eighth terms of Eq. (8) pertain to the bi-frequency plane in general. The seventh term is the response at frequency $(\omega_1+\omega_2)$; that is, $G_2(\omega_1,\omega_2)$ expresses the normalized response in the sum frequency due to non-linear interactions. Similarly, the eighth term involves response at frequency $(\omega_1-\omega_2)$; that is, $G_2(\omega_1,-\omega_2)$ is the normalized response in the difference frequency. In terms of Figure 1, the octant of the bi-frequency plane above the positive ω_1 axis corresponds to the portion of the quadratic frequency response function which defines sum-frequency interactions, and the octant below the positive ω_1 axis corresponds to the portion of the function which defines difference frequency interactions.

Equations (7) and (8) together afforded a direct way to proceed in the present investigation. In particular, what is required for a hydromechanical solution for the quadratic frequency response is to solve the hydromechanical problem for dual regular wave excitation.

GENERAL HYDRODYNAMIC FORMULATION

The initial part of the theoretical formulation is due to Salvesen[6*]. In that reference the hydrodynamic force on a body in the free surface is given as:

$$\vec{F} = -\rho \frac{d}{dt} \iint_{S_B+S_F} \Phi \, \vec{n} dS - \rho \iint_{S_B} \left[\frac{\partial \Phi}{\partial n} \nabla \Phi - \frac{1}{2} | \nabla \Phi |^2 \vec{n} \right] dS \qquad (9)$$

In the above:

$\vec{F}$ = hydrodynamic force

Φ = total velocity potential

n = outward unit normal vector

ρ = mass density

t = time

S_B = submerged surface of the body

S_F = portion of the free surface inside a far field control surface, S_∞

No approximations were made in deriving Eq. (9). The expression is taken as being exact within potential flow theory.

If it is assumed that the potential Φ is composed of a steady state wave resistance potential, Φ_S, and a time dependent potential due to waves, Φ_T,

$$\Phi = \Phi_S + \Phi_T \qquad (10)$$

---

*6. Salvesen, N., "Second-Order Steady-State Forces and Moments on Surface Ships in Oblique Regular Waves," Paper 22, International Symposium on the Dynamics of Marine Vehicles and Structures in Waves, London, April 1974.

Then Eq. (9) becomes:

$$\vec{F} = -\rho \iint_{S_B} \left[\frac{\partial \Phi_S}{\partial n} \nabla \Phi_S - \frac{1}{2} | \nabla \Phi_S |^2 \vec{n} \right] dS$$

$$-\rho \frac{d}{dt} \iint_{S_B + S_F} \Phi_T \vec{n} \, dS$$

$$-\rho \iint_{S_B} \left[\frac{\partial \Phi_S}{\partial n} \nabla \Phi_T + \frac{\partial \Phi_T}{\partial n} \nabla \Phi_S - (\nabla \Phi_S \cdot \nabla \Phi_T) \vec{n} \right] dS$$

$$-\rho \iint_{S_B} \left[\frac{\partial \Phi_T}{\partial n} \nabla \Phi_T - \frac{1}{2} | \nabla \Phi_T |^2 \vec{n} \right] dS \qquad (11)$$

In the present case the interest is in forces which are related to waves. Accordingly, the first integral in Eq. (11) may be ignored as being constant and independent of waves.

If it is assumed that the time dependent potential is linear with respect to waves, and is expressible at most in the form of sums of contributions from wave components of different frequencies, the second and third integrals make contributions to force which are also linear with waves. Under this assumption these integrals are also not of interest in the present problem.

The last integral in Eq. (11) involves products of time dependent potentials. It is thus inherently a quadratic nonlinearity even under the assumption of linear potentials. The cardinal assumption in the present work, and that of Salvesen[6], is that the dominant contribution to the quadratic or second order non-linearities comes from the combination of linear or first order potentials in the fourth integral of Eq. (11), and not from nonlinearities of the potentials themselves.

The quadratic part of the added resistance or drifting force is thus taken to be:

$$\vec{R} = -\rho \iint_{S_B} \left[\frac{\partial \Phi_T}{\partial n} \nabla \Phi_T - \frac{1}{2} | \nabla \Phi_T |^2 \vec{n} \right] dS \qquad (12)$$

where Φ_T is the first order time dependent potential. This expression is

essentially the same as that taken by Salvensen[6] in formulating the mean drifting force, and his development can be followed further.

Writing the time dependent potential as the sum of an incident wave potential, Φ_I, and a potential, Φ_B, due to the body disturbance, including diffraction effects:

$$\Phi_T = \Phi_B + \Phi_I \tag{13}$$

A result attributed to J.N. Newman is used by Salvesen to put Eq. (12) in the following form:

$$\vec{R} = \rho \iint_{S_\infty} \left[\Phi_B \frac{\partial}{\partial n} - \frac{\partial \Phi_B}{\partial n} \right] (\nabla \Phi_I + \frac{1}{2} \nabla \Phi_B) dS \tag{14}$$

Salvesen[6] made the assumption that the body is a weak scatterer so that: $\Phi_B \ll \Phi_I$. This assumption is considered to be questionable for oblique ship-wave headings. However, the assumption is considered quite reasonable for head seas (the case of present interest) and Salvesen's calculations bear this out. In order to reduce the complexity of the present analysis, the weak scattering assumption was accepted. Accordingly Eq. (14) becomes:

$$\vec{R} = \rho \iint_{S_\infty} \left[\Phi_B \frac{\partial}{\partial n} - \frac{\partial \Phi_B}{\partial n} \right] \nabla \Phi_I \, dS \tag{15}$$

This equation corresponds to Eq. (32) of Salvesen[6].

Application of Green's Theorem changes the integration in Eq. (15) to one over the body surface:

$$\vec{R} = -\rho \iint_{S_B} \left[\Phi_B \frac{\partial}{\partial n} - \frac{\partial \Phi_B}{\partial n} \right] \nabla \Phi_I \, dS \tag{16}$$

Now the present approach to the interpretation of the quadratic response function involves the computation of response to two harmonic waves of different frequencies. Given the assumption of linear potentials, this involves a simple superposition of potentials, which does not upset the conclusions made in the discussion of Eq. (11). Accordingly,

the time dependent incident and body potentials corresponding to two incident waves of frequencies ω_i and ω_j were assumed in the following form:

$$\Phi_B = \text{Re}\left[\varphi_B(\omega_i)\,\text{Exp}[-i\omega_i t] + \varphi_B(\omega_j)\,\text{Exp}[-i\omega_j t]\right]$$

$$= \frac{1}{2}\left[\varphi_B(\omega_i)\,\text{Exp}[-i\omega_i t] + \varphi_B^*(\omega_i)\,\text{Exp}[i\omega_i t]\right.$$

$$\left. + \varphi_B(\omega_j)\,\text{Exp}[-i\omega_j t] + \varphi_B^*(\omega_j)\,\text{Exp}[i\omega_j t]\right] \qquad (17)$$

$$\Phi_I = \text{Re}\left[\varphi_I(\omega_i)\,\text{Exp}[-i\omega_i t] + \varphi_I(\omega_j)\,\text{Exp}[-i\omega_j t]\right]$$

$$= \frac{1}{2}\left[\varphi_I(\omega_i)\,\text{Exp}[-i\omega_i t] + \varphi_I^*(\omega_i)\,\text{Exp}[i\omega_i t]\right.$$

$$\left. + \varphi_I(\omega_j)\,\text{Exp}[-i\omega_j t] + \varphi_I^*(\omega_j)\,\text{Exp}[i\omega_j t]\right] \qquad (18)$$

The complex potential functions $\varphi_I(\omega_k)\,\text{Exp}[-i\omega_k t]$ and $\varphi_B(\omega_k)\,\text{Exp}[-i\omega_k t]$ have the conventional interpretation in ship motions theory, they correspond to the incident and body potentials in the k^{th} regular wave train, the amplitude of the wave train is imbedded in the φ_I and φ_B functions, and the frequency ω_k is encounter frequency--not wave frequency.

Substituting Eqs. (17) and (18) into Eq. (16) and gathering terms there results:

$$\vec{R}_2 = \text{Re}\left[H_1(\omega_i,-\omega_i) + H_1(\omega_j,-\omega_j)\right]$$

$$+ \text{Re}\left[H_1(\omega_i,\omega_i)\,\text{Exp}[-i2\omega_i t]\right]$$

$$+ \text{Re}\left[H_1(\omega_j,\omega_j)\,\text{Exp}[-i2\omega_j t]\right]$$

$$+ \text{Re}\left[\left\{H_1(\omega_i,\omega_j) + H_1(\omega_j,\omega_i)\right\}\text{Exp}[-it(\omega_i+\omega_j)]\right]$$

$$+ \text{Re}\left[\left\{H_1(\omega_i,-\omega_j) + H_1^*(\omega_j,-\omega_i)\right\}\text{Exp}[-it(\omega_i-\omega_j)]\right] \qquad (19)$$

where:

$\vec{R}_2$ = force due to two superimposed regular wave trains

and:

$$H_1(\omega_i,\omega_j) = -\frac{1}{2}\iint_{S_B}\left[\rho\{\varphi_B(\omega_i)\frac{\partial}{\partial n} - \frac{\partial}{\partial n}\varphi_B(\omega_i)\}\nabla\varphi_1(\omega_j)\right]dS \qquad (20)$$

$$H_1(\omega_i,-\omega_j) = -\frac{1}{2}\iint_{S_B}\left[\rho\{\varphi_B(\omega_i)\frac{\partial}{\partial n} - \frac{\partial}{\partial n}\varphi_B(\omega_i)\}\nabla\varphi_1^*(\omega_j)\right]dS \qquad (21)$$

Now forming a new function, $H_2(\omega_i,\omega_j)$:

$$H_2(\omega_i,\omega_j) = H_1(\omega_i,\omega_j) + H_1(\omega_j,\omega_i) \qquad (22)$$

$$H_2(\omega_i,-\omega_j) = H_1(\omega_i,-\omega_j) + H_1^*(\omega_j,-\omega_i) \qquad (23)$$

This function has the same symmetries with respect to frequency arguments as the quadratic frequency response function, $G_2(\omega_1,\omega_2)$. Specifically, as in Eqs. (5) and (6):

$$H_2(\omega_j,\omega_i) = H_2(\omega_i,\omega_j)$$

and, since $\varphi_B(-\omega) = \varphi_B^*(\omega)$:

$$H_2^*(\omega_i,\omega_j) = H_2(-\omega_i,-\omega_j)$$

$$= H_2(-\omega_j,-\omega_i)$$

Substituting Eqs. (22) and (23) in Eq. (19):

$$\vec{R}_2 = \frac{1}{2}\left[H_2(\omega_i,-\omega_i) + H_2(\omega_j,-\omega_j)\right]$$

$$+ \frac{1}{2}\,\mathrm{Re}\left[H_2(\omega_i,\omega_i)\,\mathrm{Exp}[-i2\omega_i t]\right]$$

$$+ \frac{1}{2}\,\mathrm{Re}\left[H_2(\omega_j,\omega_j)\,\mathrm{Exp}[-i2\omega_j t]\right]$$

$$+ \mathrm{Re}\left[H_2(\omega_i,\omega_j)\,\mathrm{Exp}[-it(\omega_i+\omega_j)]\right]$$

$$+ \mathrm{Re}\left[H_2(\omega_i,-\omega_j)\,\mathrm{Exp}[-it(\omega_i-\omega_j)]\right] \qquad (24)$$

Thus the second order force induced by two regular wave trains has been brought into essentially the same form as the last six terms of Eq. (8).

These last six terms involve the contribution of the quadratic non-linearity in the response of the general input-output model to dual harmonic excitation.

Noting from Eq. (23) that $H_2(\omega_i,-\omega_i)$ is purely real, a comparison of Eqs. (24) and (8) yields:

$$G_2(\omega_i,-\omega_i)=\frac{1}{a_i^2}H_2(\omega_i,-\omega_i) \tag{25}$$

where a_i is the amplitude of wave component of frequency ω_i .

Continuing in the same way:

$$G_2(\omega_i,\omega_i) = \frac{1}{a_i^2}H_2^*(\omega_i,\omega_i) \tag{26}$$

$$G_2(\omega_i,\omega_j) = \frac{1}{a_i a_j}H_2^*(\omega_i,\omega_j) \tag{27}$$

and:

$$G_2(\omega_i,-\omega_j) = \frac{1}{a_i a_j}H_2^*(\omega_i,-\omega_j) \tag{28}$$

Thus the formulation of the computation of the quadratic frequency response function is complete. For each pair of regular waves of amplitudes a_i and a_j, and frequencies ω_i and ω_j, Eqs. (20) and (21) must be evaluated to form $H_1(\omega_i,\omega_j)$, $H_1(\omega_j,\omega_i)$, $H_1(\omega_i,-\omega_j)$ and $H_1(\omega_j,-\omega_i)$. From these results Eqs. (22), (23), (27) and (28) may be evaluated in turn to yield the desired estimates.

One observation is in order before continuing. The present development involves relatively little specialization to added resistance. Computation of quadratic frequency response functions may be made according to the above recipe for other forces within the assumption of linearized potential flow for a body which may be considered a weak scatterer. Removal of the weak scattering assumption appears feasible at the expense of a moderate increase in complexity of the resulting hydrodynamic expressions.

Finally, it is of interest to compare the present result with the corresponding stage in Salvesen's development for the mean force induced by a single wave. To do this let the amplitude of the j^{th} wave component go to zero. Since the amplitude is imbedded in the potentials:

$\varphi_B(\omega_j) = \varphi_I(\omega_j) = 0$ and thus only the first and third terms remain in Eq. (19). Taking the time mean of the first and third terms of Eq. (19) leaves only the first term:

$$\mathrm{Re}[H_1(\omega_i, -\omega_i)]$$

Apart from the explicit notation that the real part is to be taken, and some purely notational differences, this result is exactly the same as Salvesen's Eq. (34) for the mean force.

ANALYTICAL EVALUATION OF THE QUADRATIC FREQUENCY RESPONSE FUNCTION FOR ADDED RESISTANCE

While there is no fundamental objection to the development of a vector quadratic frequency response function corresponding to the vector force represented by the equations of the last section, the objectives of the present work involved only a comparison with experimental results for added resistance in head seas, and it was accordingly a worth-while simplification to consider only the longitudinal component of force for the head sea case.

In general, the evaluation of the functions, Eqs. (20) and (21), was carried out in a manner similar to that employed by Salvesen[6] in that a strip method was used, and the same or very similar hydrodynamic assumptions were employed. Some differences do exist because the strip method used was that of Ref. 7.*

The most important difference between this method and others (Ref. 6 for example) is in the evaluation of the diffraction induced wave exciting forces and moments. The method of Ref. 7 is essentially an extension to forward speed of the method for zero speed developed in Ref. 8. In both, the diffraction induced forces and moments as well as the motion induced forces and moments are evaluated by the Frank[9] close fit method. Because the work of Ref. 7 has not as yet received wide circulation, a summary of the method is included herein as Appendix A.

---

*7. Kim, C.H., "Calculation of Motions and Loads of a Ship Uniformly Advancing in Oblique Regular Waves," Technical Memorandum SIT-DL-74-166, March 1974.

8. Kim, C.H. and Chou, F., "Wave-Exciting Forces and Moments on an Ocean Platform in Oblique Seas," Paper No. OTC 1180, Offshore Technology Conference, April 1970. Also SIT-OE-71-Report 6, September 1971.

9. Frank, W., "On the Oscillation of Cylinders in or Below the Free Surface of Deep Fluids," NSRDC Report 2375, October 1967.

Figure 2 indicates the usual right-handed coordinate system used in the present development. It is described in more detail in Appendix A. In the present case the ship is presumed to be restrained in surge and to be proceeding at constant velocity U in two superimposed head waves ($\mu = \pi$ in Figure 2).

In a manner consistent with the form of the incident wave potential assumed in Eq. (18), the two regular waves are represented by the real parts of:

$$\zeta_i = a_i e^{-i(\nu_{o_i} x + \omega_i t)}$$

and:

$$\zeta_j = a_j e^{-i(\nu_{o_j} x + \omega_j t)} \tag{29}$$

Here the i,j subscripts indicate two different waves, and

a_i = wave amplitude

$\nu_{o_i} = \omega_{oi}^2/g$, the wave number

$\omega_i = \omega_{o_i} + U\nu_{o_i}$, frequency of encounter

The incident wave potential, $\varphi_I(\omega_j)$, for the j^{th} head wave train is given by (omitting the time factor in accordance with Eq. 18):

$$\varphi_I(\omega_j) = -i \frac{ga_j}{\omega_{o_j}} e^{\nu_{o_j}(z-ix)} \tag{30}$$

The gradient of the incident potential for the j^{th} wave is:

$$\nabla\varphi_I(\omega_j) = [\vec{i}(-i\nu_{o_j}) + \vec{k}\nu_{o_j}]\varphi_I(\omega_j) \tag{31}$$

In order to specialize the analysis to added resistance, only the longitudinal component of Eq. (31) is taken. Accordingly, in the evaluation of Eqs. (20) and (21) the gradients of the incident wave potentials may be replaced as follows:

$$\nabla\varphi_I(\omega_j) \rightarrow -i\nu_{o_j}\varphi_I(\omega_j)$$

$$\nabla\varphi_I^*(\omega_j) \rightarrow i\nu_{o_j}\varphi_I^*(\omega_j) \tag{32}$$

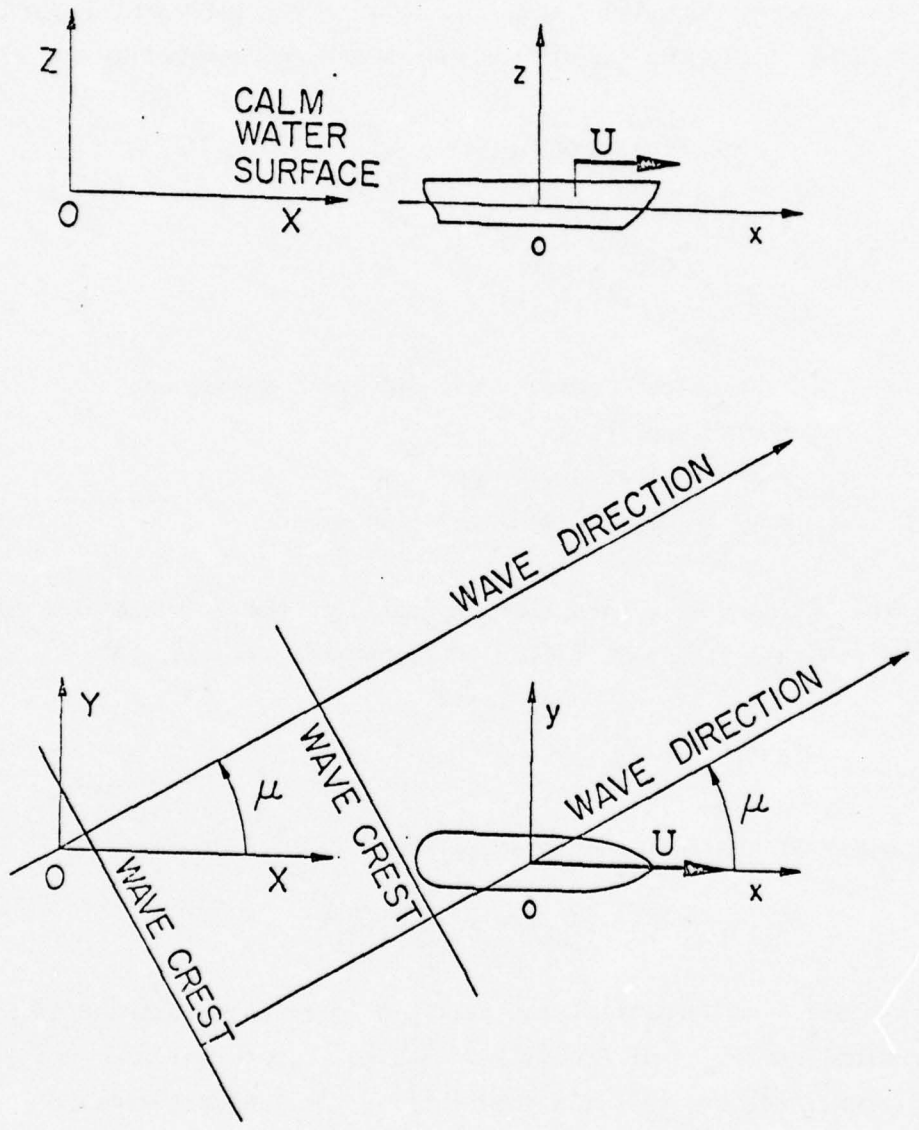

FIGURE 2 THE COORDINATE SYSTEM

with the understanding that the result will apply only to the longitudinal component of force.

The body potential for the i^{th} wave train is taken as the sum of the radiation and diffraction potentials. Because of the heading, only vertical modes of motion are considered. Thus for the response to the i^{th} wave train:

$$\varphi_B(\omega_i) = \sum_{m=3,5} V^{(m)}(\omega_i)\varphi^{(m)}(\omega_i) + a_i\varphi_D(\omega_i)e^{-i\nu_{o_i}x} \tag{33}$$

where:

$V^{(m)}(\omega_i)$ = velocity amplitude of heave (m=3) and pitch (m=5)

$\varphi^{(m)}(\omega_i)$ = radiation potential due to heaving and pitching motions, each per unit velocity amplitude

$\varphi_D(\omega_i)$ = the diffraction potential per unit wave amplitude in the i^{th} wave train (see Appendix A)

$$V^{(3)}(\omega_i) = -i\omega_i\zeta(\omega_i)$$

$$V^{(5)}(\omega_i) = -i\omega_i\psi(\omega_i) \tag{34}$$

and ζ and ψ indicate the heave and pitch displacement, respectively.

The diffraction potential for the i^{th} wave train, φ_D, (Appendix A) is evaluated by satisfying the kinematical boundary condition:

$$\frac{\partial}{\partial n}\left[a_i\varphi_D(\omega_i)e^{-i\nu_{o_i}x}\right] = -\frac{\partial}{\partial n}\varphi_I(\omega_i) \qquad \text{on } S_B \tag{35}$$

Substititing Eqs. (32), (33), and (35) into Eqs. (20) and (21) there results:

$$H_1(\omega_i,\omega_j) = \frac{1}{2}\nu_{o_j}\rho\Big\{\sum_{m=3,5} V^{(m)}(\omega_i)\iint_{S_B}\varphi^{(m)}(\omega_i)\frac{\partial\varphi_1(\omega_j)}{\partial n}\,dS$$

$$+ a_i\iint_{S_B}\varphi_D(\omega_i)e^{-i\nu_{o_i}x}\frac{\partial\varphi_1(\omega_j)}{\partial n}\,dS$$

$$-\sum_{m=3,5} V^{(m)}(\omega_i)\iint_{S_B}\frac{\partial\varphi^{(m)}(\omega_i)}{\partial n}\varphi_1(\omega_j)\,dS$$

$$+\iint_{S_B}\frac{\partial\varphi_1(\omega_i)}{\partial n}\varphi_1(\omega_j)\,dS\Big\} \qquad (36)$$

$$H_1(\omega_i,-\omega_j) = \frac{1}{2}\nu_{o_j}\rho\Big\{-\sum_{m=3,5} V^{(m)}(\omega_i)\iint_{S_B}\varphi^{(m)}(\omega_i)\frac{\partial\varphi_1^*(\omega_j)}{\partial n}\,dS$$

$$- a_i\iint_{S_B}\varphi_D(\omega_i)e^{-i\nu_{o_i}x}\frac{\partial\varphi_1^*(\omega_j)}{\partial n}\,dS$$

$$+\sum_{m=3,5} V^{(m)}(\omega_i)\iint_{S_B}\frac{\partial\varphi^{(m)}(\omega_i)}{\partial n}\varphi_1^*(\omega_j)\,dS$$

$$-\iint_{S_B}\frac{\partial\varphi_1(\omega_i)}{\partial n}\varphi_1^*(\omega_j)\,dS\Big\} \qquad (37)$$

In the radiation problem the kinematical boundary conditions for heaving and pitching are given by

$$\frac{\partial\varphi^{(3)}}{\partial n} = \underline{n}$$

$$\frac{\partial\varphi^{(5)}}{\partial n} = -\underline{n}\left(x + \frac{U}{i\omega_i}\right) \qquad \text{on } S_B \qquad (38)$$

where $\underline{n}$ is the z-component of the unit normal on the hull surface (in fact, it is on a section surface in the stripwise calculation) pointing into the water.

From the above we have the relationship between $\varphi^{(3)}$ and $\varphi^{(5)}$,

$$\varphi^{(5)}(\omega_i) = -(x + \frac{U}{i\omega_i})\varphi^{(3)}(\omega_i) \tag{39}$$

The partial of the incident wave potential is evaluated as:

$$\frac{\partial \varphi_I(\omega_j)}{\partial n} = \underline{n}\nu_{o_j}\varphi_I(\omega_j) \tag{40}$$

where in the slender body approximation the x-component of the unit normal is zero.

Further, from Eq. (38):

$$\omega_i \frac{\partial \varphi^{(m)}(\omega_i)}{\partial n} = \omega_i n^{(m)} + iUm^{(m)} \tag{41}$$

where

$$n^{(3)}=\underline{n},\ n^{(5)}=-\underline{n}x,\ m^{(3)}=0,\ m^{(5)}=\underline{n} \tag{42}$$

according to the variant of Stokes' theorem,[6] we have:

$$\iint_{S_B} \omega_i \frac{\partial \varphi^{(m)}(\omega_i)}{\partial n} \varphi_I(\omega_j)\,dS = \iint_{S_B} (\omega_i n^{(m)} + iUm^{(m)})\varphi_I(\omega_j)\,dS \tag{43}$$

It may be seen that substitution of Eq. (40) through (43) in Eqs. (36) and (37) results in a factor of $\underline{n}$ in each term. Accordingly the double integral over S_B in the equations may be replaced by a strip-wise integration:

$$\iint_{S_B} \underline{n}\,dS = -\int_L dx \int_{C(x)} dy \tag{44}$$

where $C(x)$ = a transverse section contour

y = a transverse coordinate

L = hull length

Further transformations of the terms in Eqs. (36) and (37) are effected as follows: The sectional heave added mass $m''(\omega_i)$ and damping coefficient $N(\omega_i)$ are obtained from the following relation,

$$\rho\omega_i \int_{C(x)} \varphi^{(3)}(\omega_i)dy = \omega_i m''(\omega_i) + iN(\omega_i) \tag{45}$$

The sectional heave diffraction force per unit wave amplitude (see Appendix A) is given by:

$$i\rho\omega_i \int_{C(x)} \varphi_D(\omega_i)dy = f_H^D(\omega_i) \tag{46}$$

The sectional restoring force per unit heave displacement is given by:

$$\rho g \int_{C(x)} dy = \rho g B \tag{47}$$

where B = beam of the section in the load waterplane.

By taking the average section draft $\bar{T}$ at x in the integral of the exponential, an approximate expression can be derived:

$$\int_{C(x)} e^{\nu_{o_j} z}\, dy = e^{-\nu_{o_j} \bar{T}} \int_{C(x)} dy \tag{48}$$

where $\bar{T} = \dfrac{\text{wetted sectional area}}{\text{wetted section beam}}$

Upon substitution of Eqs. (30), (34), (38) through (40), and (43) through (48) into Eqs. (36) and (37) there resulted expressions which could be evaluated with the aid of existing ship motion programs.[7]

$$H_1(\omega_i,\omega_j) =$$

$$\frac{i}{2} a_i a_j \nu_{o_j} \omega_{o_j} \left\{ \frac{\zeta(\omega_i)}{a_i} \int_L e^{-i\nu_{o_j} x} e^{-\nu_{o_j} \bar{T}} [\omega_i m''(\omega_i) + iN(\omega_i)] dx \right.$$

$$\left. - \frac{\psi(\omega_i)}{a_i} \int_L (x + \frac{U}{i\omega_i}) e^{-i\nu_{o_j} x} e^{-\nu_{o_j} \bar{T}} [\omega_i m''(\omega_i) + iN(\omega_i)] dx \right\}$$

$$+ \frac{i}{2} a_i a_j \nu_{o_j} \frac{\omega_{o_j}}{\omega_i} \int_L e^{-i(\nu_{o_i} + \nu_{o_j}) x} e^{-\nu_{o_j} \bar{T}} f_H^D(\omega_i) dx$$

$$+ \frac{i}{2} a_i a_j \nu_{o_j} \left[-1 + \frac{\omega_i + \omega_j}{\omega_{o_j}} \right]$$

$$\left\{ - \frac{\zeta(\omega_i)}{a_i} \int_L e^{-i\nu_{o_j} x} e^{-\nu_{o_j} \bar{T}} \rho g B \, dx \right.$$

$$\left. + \frac{\psi(\omega_i)}{a_i} \int_L x e^{-i\nu_{o_j} x} e^{-\nu_{o_j} \bar{T}} \rho g B \, dx \right\}$$

$$+ \frac{i}{2} a_i a_j \frac{\omega_{o_i} \omega_{o_j}}{g} \int_L e^{-i(\nu_{o_i} + \nu_{o_j}) x} e^{-(\nu_{o_i} + \nu_{o_j}) \bar{T}} \rho g B \, dx \quad (49)$$

$$H_1(\omega_i,-\omega_j) =$$

$$\frac{i}{2} a_i a_j \nu_{o_j} \omega_{o_j} \left\{ \frac{\zeta(\omega_i)}{a_i} \int_L e^{i\nu_{o_j} x} e^{-\nu_{o_j} \bar{T}} [\omega_i m''(\omega_i) + iN(\omega_i)]dx \right.$$

$$\left. - \frac{\psi(\omega_i)}{a_i} \int_L (x + \frac{U}{i\omega_i}) e^{i\nu_{o_j} x} e^{-\nu_{o_j} \bar{T}} [\omega_i m''(\omega_i) + iN(\omega_i)]dx \right\}$$

$$+ \frac{i}{2} a_i a_j \nu_{o_j} \frac{\omega_{o_j}}{\omega_i} \int_L e^{-i(\nu_{o_i} - \nu_{o_j})x} e^{-\nu_{o_j} \bar{T}} f_H^D(\omega_i)dx$$

$$+ \frac{i}{2} a_i a_j \nu_{o_j} \left[1 + \frac{\omega_i - \omega_j}{\omega_{o_j}} \right]$$

$$\left\{ - \frac{\zeta(\omega_i)}{a_i} \int_L e^{i\nu_{o_j} x} e^{-\nu_{o_j} \bar{T}} \rho g B \, dx \right.$$

$$\left. + \frac{\psi(\omega_i)}{a_i} \int_L x e^{i\nu_{o_j} x} e^{-\nu_{o_j} \bar{T}} \rho g B \, dx \right\}$$

$$+ \frac{i}{2} a_i a_j \frac{\omega_{o_i} \omega_{o_j}}{g} \int_L e^{-i(\nu_{o_i} - \nu_{o_j})x} e^{-(\nu_{o_i} + \nu_{o_j})\bar{T}} \rho g B \, dx \quad (50)$$

For present purposes the expressions (Eqs. 49 and 50) for $H_1(\omega_i,\omega_j)$ and $H_1(\omega_i,-\omega_j)$ may be used in place of Eqs. (20) and (21) in the expressions for $H_2(\omega_i,\omega_j)$, etc., Eqs. (22) and (23), with the understanding that the result relates only to the quadratic frequency response function for the longitudinal component of force. Equations (49) and (50) contain the product of the regular wave amplitudes $(a_i a_j)$ as a factor. Thus the functions $H_2(\omega_i,\omega_j)$, Eqs. (22) and (23), have the same factor, and when the quadratic frequency response function is evaluated by Eqs. (25) through (28) the factor cancels -- meaning that Eqs. (49) and (50) may be evaluated for unit wave amplitudes.

The dimension of the quadratic frequency response function is (force/length^2). In the reduction of experimental data (Ref. 1-5) length was non-dimensionalized with model length, L, forces were non-dimensionalized with model displacement, Δ, resistance was considered to be a

positive force, and frequency was non-dimensionalized with $\sqrt{2\pi g/L}$. Thus the last details in generating theoretical estimates comparable to those in Refs. 1-5 are to change the sign of the results of Eqs. (25) through (28) and multiply by L^2/Δ, and compensate for the frequency non-dimensionalizing constant.

As may be noted from Eqs. (22) and (23), the answer sought for bi-frequency ω_i, ω_j involves the evaluation of Eqs. (49) and (50) as written, and with the i j subscripts interchanged. In addition, it was required to develop the theoretical estimates over a region in the ω_1, ω_2 plane, Figure 1. This means that results from the basic ship motions computation for each frequency must be used over and over again. Accordingly the actual computation was divided into two steps. Before commencing the first step the required extent and fineness of coverage of the bi-frequency plane are decided upon, and a value of $\delta\omega$ and K are chosen. These parameters define the discrete points in the plane at which estimates of the quadratic frequency response will be generated; that is, estimates are thus specified to be made for all combinations of:

$$\omega_1 = 0, \delta\omega, \cdots K\delta\omega$$

$$\omega_2 = -K\delta\omega, \cdots, -\delta\omega, 0, \delta\omega \cdots K\delta\omega$$

Given a forward ship speed, U, the wave numbers corresponding to each of the (K+1) encounter frequencies may be solved for.

In the first step of the computation the ship motions problem is solved for each of the (K+1) discrete encounter frequencies. Essentially, the sectional added mass, damping, restoring force and exciting force are developed for each strip and these are integrated to result in estimates of pitch and heave amplitudes. All of these results are stored so that the result of the first computational step is a "library" of sectional added mass, damping, etc., for all the specified encounter frequencies. Results for "zero" frequency are approximated by those for a very low frequency.

In the second step of the computation Eqs. (49) and (50) are systematically evaluated for each combination of the discrete frequencies

by "looking up" the previously computed data from the first computational step, and the estimation of the quadratic frequency response continues in accordance with Eqs. (22), (23) and (25) through (28).

COMPARISON OF ANALYTICAL AND EXPERIMENTAL ESTIMATES OF THE MEAN ADDED RESISTANCE OPERATOR

As previously noted, the mean added resistance operator is the value of the quadratic frequency response function along the line $\omega_2 = -\omega_1$, and it is this special section of the function for which there is a great deal of confirming information. Thus the initial comparisons with experiment of the present analytical method were of the mean operator. The model used in the experiments of Ref. 1-5 was of the Series 60 0.60 C_B parent, and this model was also one of those used in experiments reported by Strom-Tejsen, et al[10*].

Figure 3 shows results from the present analysis plotted on what is effectively Figure 8a of Ref. 10. The work in Ref. 10 on the Series 60, 0.60 block model had involved two speeds (Froude numbers 0.266 and 0.283). The evaluation of the present analytical method was carried out at the mean of the two speeds, $F_n = 0.274$, and the results were non-dimensionalized in accordance with the conventions employed in Ref. 10. The present results are clearly closer to experiment for this case than are the results of the analytical methods of Ref. 10. In addition, at high encounter frequencies the present method indicates the leveling out trend often observed in experimental added resistance operators.

The experimental work in Refs. 1-5 had also involved two speeds, $F_n = 0.15$ and 0.20. The lower of the two speeds was selected and the quadratic frequency response function was evaluated. For this case Figure 4 indicates the comparison with experiment of the mean added resistance operator from the present analytical method. Except for the addition of the analytical result, Figure 4 is also Figure 4 of Ref. 1 or Figure 2 of Ref. 5. In this figure the σ_e is a non-dimensional encounter frequency:

$$\sigma_e = \omega_e / \sqrt{2\pi g / L}$$

where ω_e is encounter frequency in radians/second.

---

*10. Strom-Tejsen, J., Yeh, H.Y.H., and Moran, D.D., "Added Resistance in Waves," SNAME Vol. 81, pp 109, 1973.

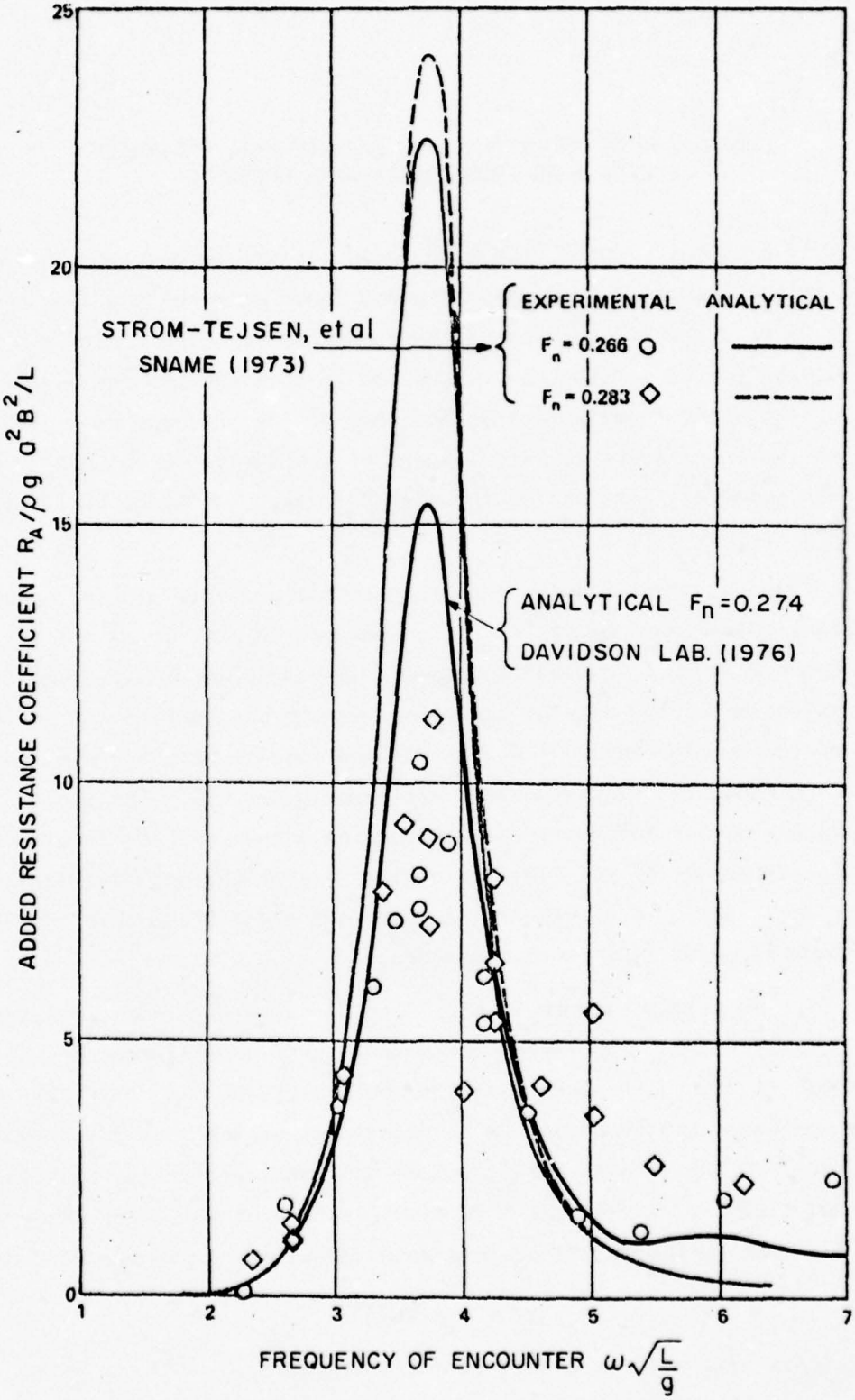

FIGURE 3 COMPARISON OF ANALYTICAL AND EXPERIMENTAL MEAN ADDED RESISTANCE OPERATORS, DATA FROM REFERENCE 10

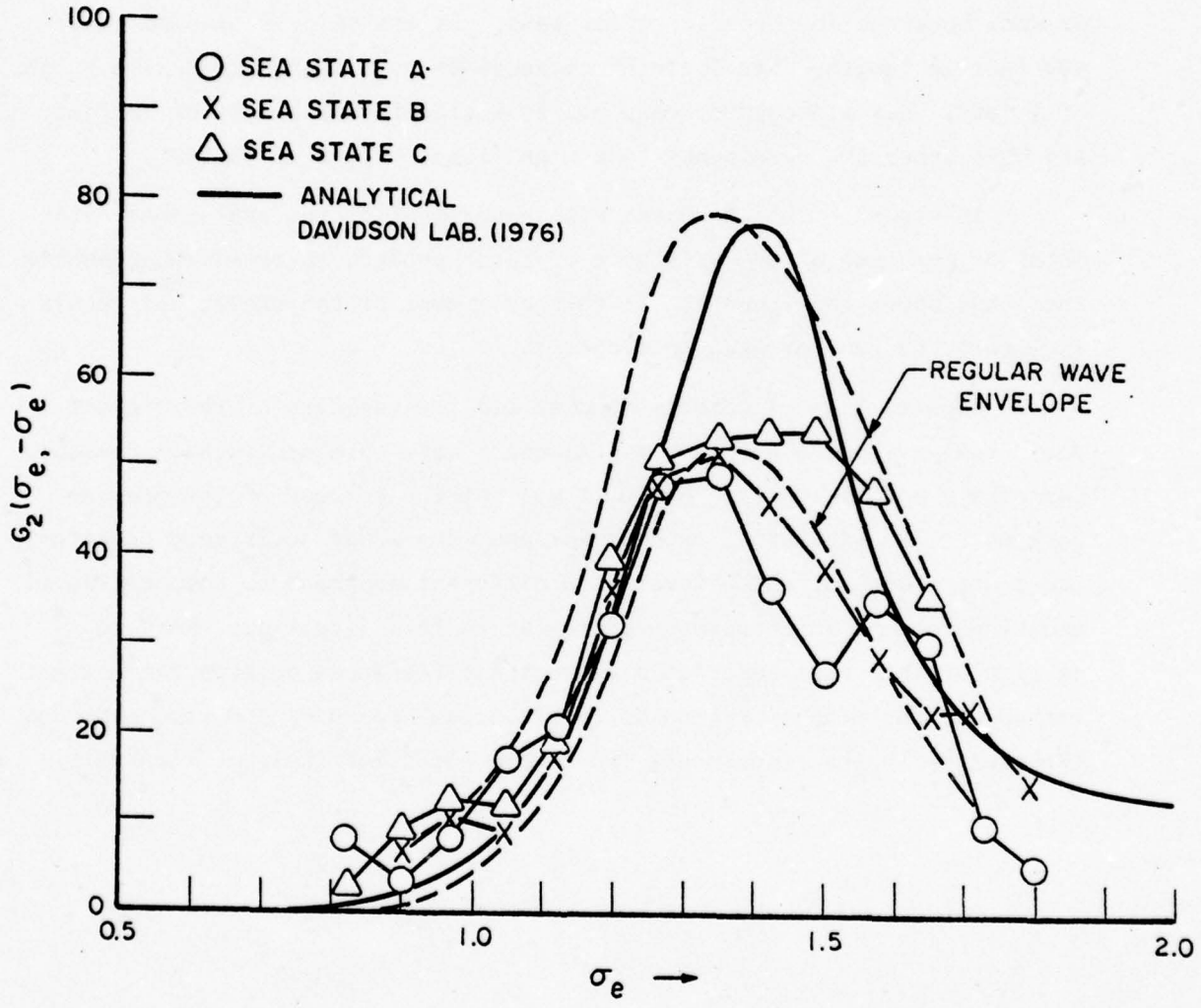

FIGURE 4 COMPARISON OF ANALYTICAL AND EXPERIMENTAL MEAN ADDED RESISTANCE OPERATORS, DATA FROM REFERENCES 1 AND 2

The added resistance operator is non-dimensionalized by L^2/Δ as noted in the previous section. Two kinds of experimental data are included in the figure. The regular wave envelope indicates the magnitude and scatter of the results of regular wave experiments reported in Ref. 2. The lines broken by various symbols are the results of cross-bi-spectral analyses of data obtained in three irregular seas. If the ship is assumed to be 500 feet in length, "Sea State A" corresponds to a significant wave height of 9 feet, "Sea State B" corresponds to a significant height of 18 feet, and "Sea State C" corresponds to a significant height of 33 feet.

In Figure 4 the agreement with experiment of the analytical estimates of the mean added resistance operator appears to be somewhat better than that shown in Figure 3. In this case most of the analytical result is within the regular wave envelope.

Figures 3 and 4 clearly demonstrate the validity of the present analytical method relative to experimental data obtained both at Davidson Laboratory and elsewhere. While it was not the purpose of the present work to refine estimating methods for the mean added resistance operator, the present method, which involves a different approach to computation of exciting forces, appears to have promise in this direction. For the particular ship form and speeds shown, the differences between the present method and the mean experimental result appear to be of the same order as the scatter in the experiments (which are noted for their difficulty).

COMPARISON OF ANALYTICAL AND EXPERIMENTAL ESTIMATES OF THE QUADRATIC FREQUENCY RESPONSE FUNCTION

In order to compare the analytical estimates of the complete quadratic frequency response function with those from experiment it is advantageous to introduce the frequency transformation of Ref. 1. This transformation maps the ω_1, ω_2 plane (Fig.1) into a sum and difference frequency plane in accordance with:

$$\Omega_1 = \omega_1 - \omega_2 = \text{difference frequency}$$
$$\Omega_2 = \omega_1 + \omega_2 = \text{sum frequency} \qquad (51)$$

The Ω_1, Ω_2 plane is shown mapped into the ω_1, ω_2 plane in Figure 5. The Ω_1 and Ω_2 axes are coincident with the lines of symmetry noted in the discussion of Figure 1. In accordance with the discussion of Figure 1 the fundamental symmetry of the quadratic frequency response function allows complete definition if the function is known in a quadrant of the plane defined by the lines of symmetry. The quadrant of the Ω_1, Ω_2 plane (Fig.5) in which both sum and difference frequencies are positive corresponds to the quadrant selected earlier in interpreting the response to dual harmonic excitation. This quadrant will be used in the comparsions. Also in accordance with the earlier discussion of dual harmonic excitation, the sum frequency, Ω_2 corresponds, and is numerically equal to, the output frequency. Any combination of input frequencies ω_1 and ω_2 which are on the line Ω_2 = constant will generate a component at that frequency. For example, the mean added resistance operator involves output frequency of zero and is located on the Ω_1 axis.

For comparison purposes the frequency transformation involves no changes to the magnitude of the analytical estimates of the quadratic frequency response function, merely a somewhat more convenient way of looking at the function. The analytical results for the Series 60 0.60 block model at Froude Number of 0.15 were non-dimensionalized in accordance with the experimental convention noted in a previous section.

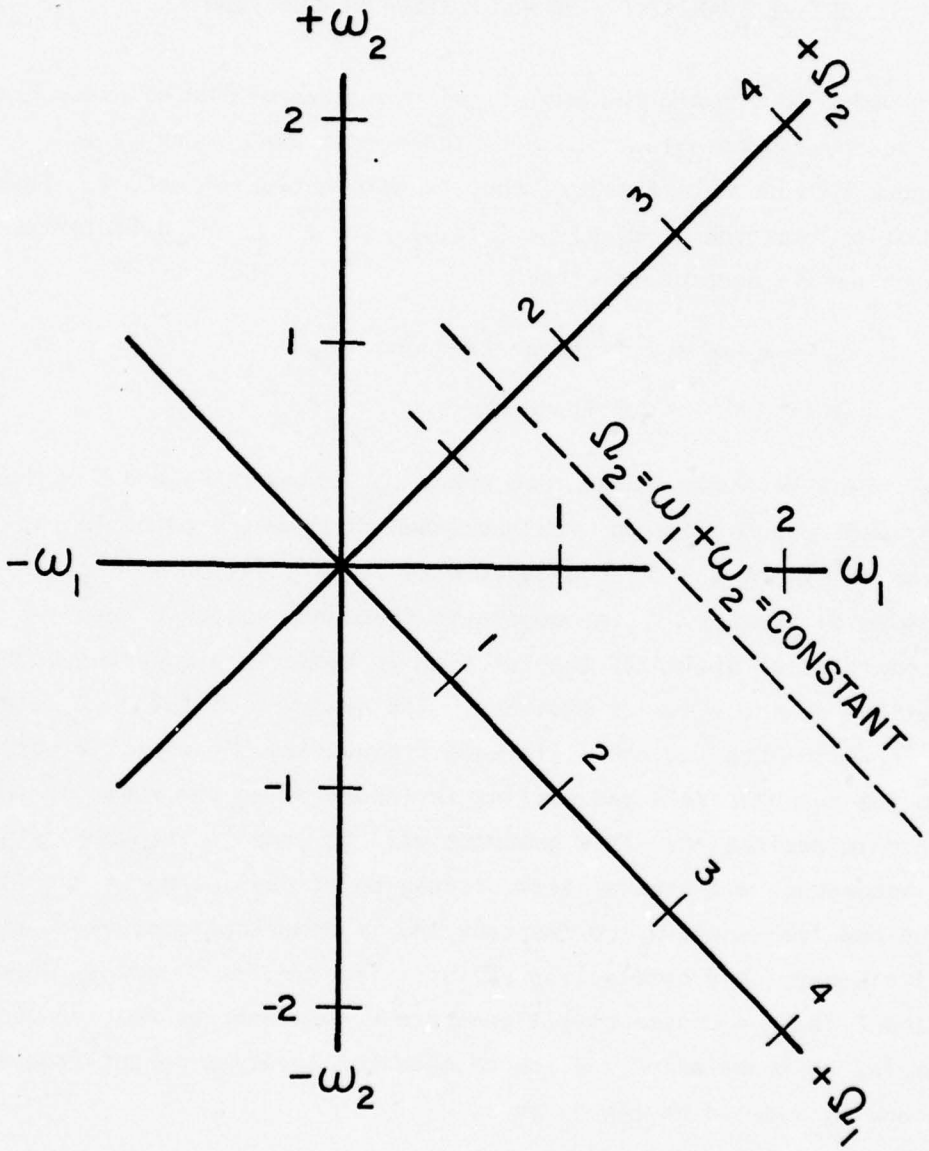

FIGURE 5 MAPPING OF THE Ω_1, Ω_2 PLANE

The discrete set of frequencies at which the function was evaluated were chosen so that results would be available for the exact non-dimensional frequencies used in the experimental identification process. The non-dimensional frequencies are denoted in Ref. 1 by σ_1 and σ_2 instead of ω_1 and ω_2. Since the σ's differ from the ω's only by a scale factor σ_1 and σ_2 may be substituted for ω_1 and ω_2 in Eq. (51) and in fact in all previous equations. For present purposes, however, ω_1 and ω_2 will be taken to denote non-dimensional frequency.

Before proceeding with detailed comparisons an overview of the magnitude of the analytical result is instructive. Figure 6 is an isometric plot of the modulus of the analytically determined quadratic frequency response function. The "view" is toward the origin of the bi-frequency plane from a position above the ω_1 axis, Figure 5. (The difference frequency axis (Ω_1) is to the left, the sum frequency axis is to the right, and the modulus of the function is "vertical".) The lines defining the function contours are in the nature of section lines which are parallel to the Ω_1 and Ω_2 axes. Each intersection corresponds to an analytically computed point, and the connecting line segments are straight. There were actually about twice as many points computed as are shown. It is a consequence of the point spacing chosen for plotting that the function appears to be irregular near maxima. Inspection of the intermediate numerical results indicated that the computation defines a smooth surface. In the figure the plotted domain of the bi-frequency plane appears triangular. This is the result of computing the function to a maximum absolute input frequency of 2.62. The right-to-left section at the front of the plot is shown in bolder lines with vertical lines defining the position of computed points. This section represents the modulus of the function along the line $\omega_1 = 2.62$.

Qualitatively Figure 6 shows that the modulus of the analytical quadratic frequency response function resembles that expected; that is, there are two prominent humps, one associated with difference frequency interactions, one associated with sum frequency interactions, and in addition the two humps are not symmetrical. At bi-frequencies distant from those of the main humps the modulus of the function is higher than

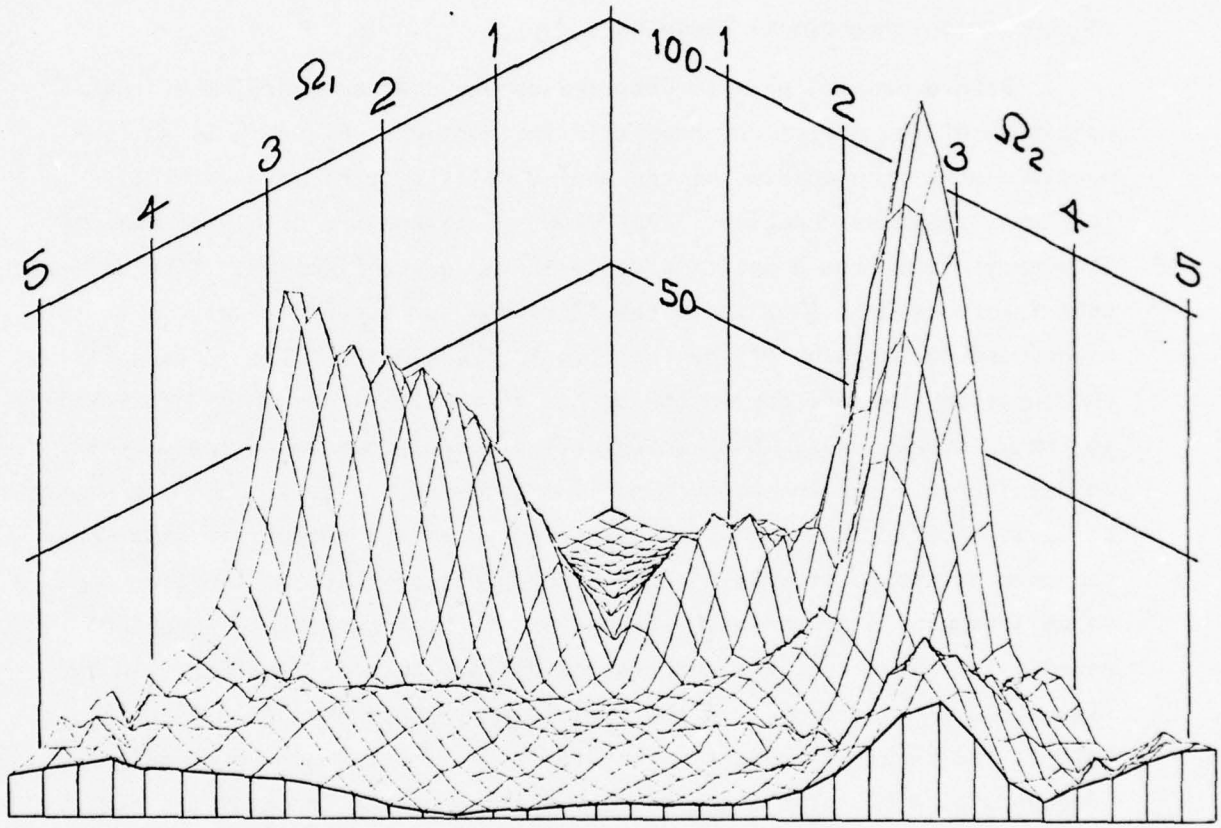

FIGURE 6 ISOMETRIC VIEW OF THE MODULUS OF THE ANALYTICALLY ESTIMATED QUADRATIC FREQUENCY RESPONSE FUNCTION

was expected (though it must be admitted that the expectation was not based on firm experimental estimates). Clearly, the maximum input frequency should have been extended beyond $\omega_1 = 2.62$ for purposes of better defining the bi-frequency domain of significance. This additional computation was not carried out because no experimental results were available for the corresponding bi-frequencies.

The experimental estimates as presented in Ref. 1 are not quite equivalent to the analytical estimates by reason of a difference in phase reference point. The phases in the analytical estimates are with reference to wave at LCG. The phases in the experimental results are with respect to a wave one model length forward of LCG which had been time shifted to aid in the cross-bi-spectral analysis process. Within the objectives of Ref. 1 it was convenient to retain this peculiar phase reference. For present purposes it was convenient to correct the experimental results to the same phase reference as had been assumed for the analytical case. The net phase difference between the time shifted wave and wave at LCG was calculated according to the outline in Ref. 2. This net difference is equivalent to a linear filter with unity modulus acting upon the input to the system, and the experimental quadratic frequency response function estimates were corrected according to the rules in Refs. 1 and 5 for cascaded linear and quadratic systems.

The qualitative indications mentioned in connection with Figure 6 suggested that an initial comparison between the magnitude of analytical and experimental estimates might best becarried out indirectly. The experimental estimates were made from the ratio of two cross-bi-spectral estimates in accordance with:

$$\hat{G}_2(\omega_1,\omega_2) = \hat{G}_2\left(\frac{\Omega_1+\Omega_2}{2}, \frac{\Omega_2-\Omega_1}{2}\right)$$
$$= C_D^*(\Omega_1,\Omega_2)/C_\eta(\Omega_1,\Omega_2) \qquad (52)$$

where the cap denotes an estimate and:

$C_D^*(\Omega_1,\Omega_2)$ is the cross-bi-spectrum of wave, wave and resistance

$C_\eta(\Omega_1,\Omega_2)$ is the cross-bi-spectrum of wave, wave and $(\text{wave})^2$.

Since:

$$C_\eta(\Omega_1,\Omega_2) = S_{\eta\eta}(\omega_1)S_{\eta\eta}(\omega_2)$$

where

$S_{\eta\eta}(\omega)$ is the scalar spectrum of wave,

the wave,wave,$(\text{wave})^2$ cross-bi-spectrum is just another way of estimating the product of scalar wave spectra. When $C_\eta(\Omega_1,\Omega_2)$ is small the excitation of the system at that bi-frequency is small, and the estimates implied by Eq. (52) may be expected to be seriously corrupted by noise. In Refs. 1 and 5 estimates resulting from Eq. (52) where $C_\eta(\Omega_1,\Omega_2)$ was less than 10% of its peak were discarded. Figure 7 is an isometric plot of one of the experimental wave,wave,$(\text{wave})^2$ cross-bi-spectra. This cross-bi-spectrum (and those for the other experimental sea states) is very small in much of the bi-frequency plane.

These considerations suggested that a first comparison of analysis and experiment should be made by computing the wave,wave,resistance cross-bi-spectrum which should have been observed by experiment, given the analytical results for the quadratic frequency response function and the experimental wave spectrum or the experimental results for $C_\eta(\Omega_1,\Omega_2)$. The computation for the modulus of the wave,wave,resistance cross-bi-spectrum for experimental Sea State B for instance, amounts to multiplying the function shown in Figure 6 by that shown in Figure 7, or:

$$|C_{DT}(\Omega_1,\Omega_2)| = |G_{2T}(\tfrac{\Omega_1+\Omega_2}{2}, \tfrac{\Omega_2-\Omega_1}{2})|\,|C_\eta(\Omega_1,\Omega_2)| \qquad (53)$$

in which the subscripts "T" denote analytical estimates. This procedure has the effect of weighting the analytical estimates so that quadratic response which should not have been excited in the experiments does not enter in the comparisons.

The computation defined by Eq. (53) was carried out for each of the three experimental sea-states. These "analytically" estimated cross-bi-spectra are shown along with the corresponding experimental cross-bi-spectra in Figures 8 through 10 in isometric views having the same conventions as Figure 6. At the top of each figure is the analytical prediction.

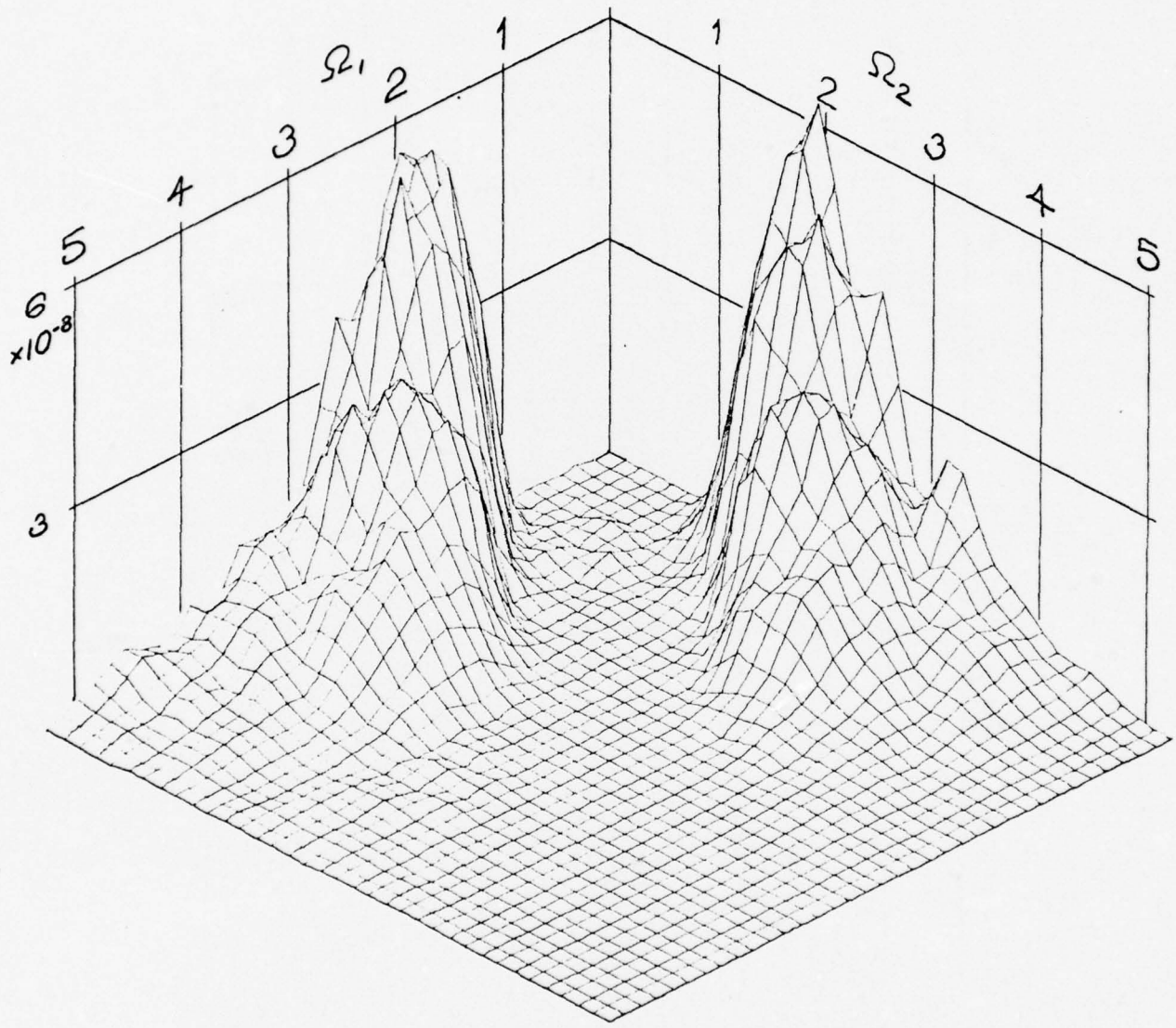

FIGURE 7 THE WAVE, WAVE, $(\text{WAVE})^2$ CROSS-BI-SPECTRUM FOR SEA STATE B

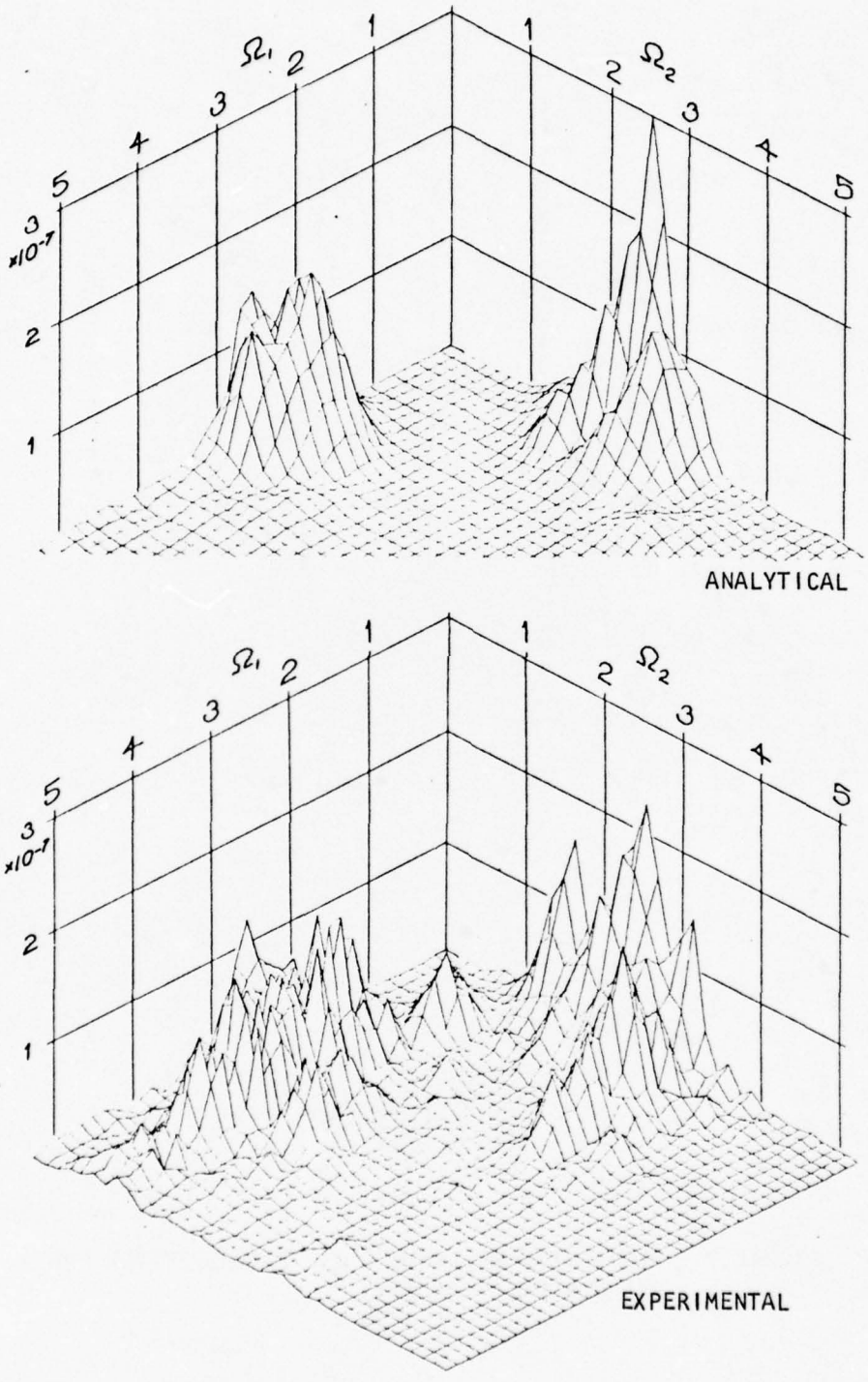

FIGURE 8 ANALYTICALLY PREDICTED AND EXPERIMENTALLY DERIVED CROSS-BI-SPECTRAL MODULI: FROUDE NUMBER 0.15, SEA STATE A

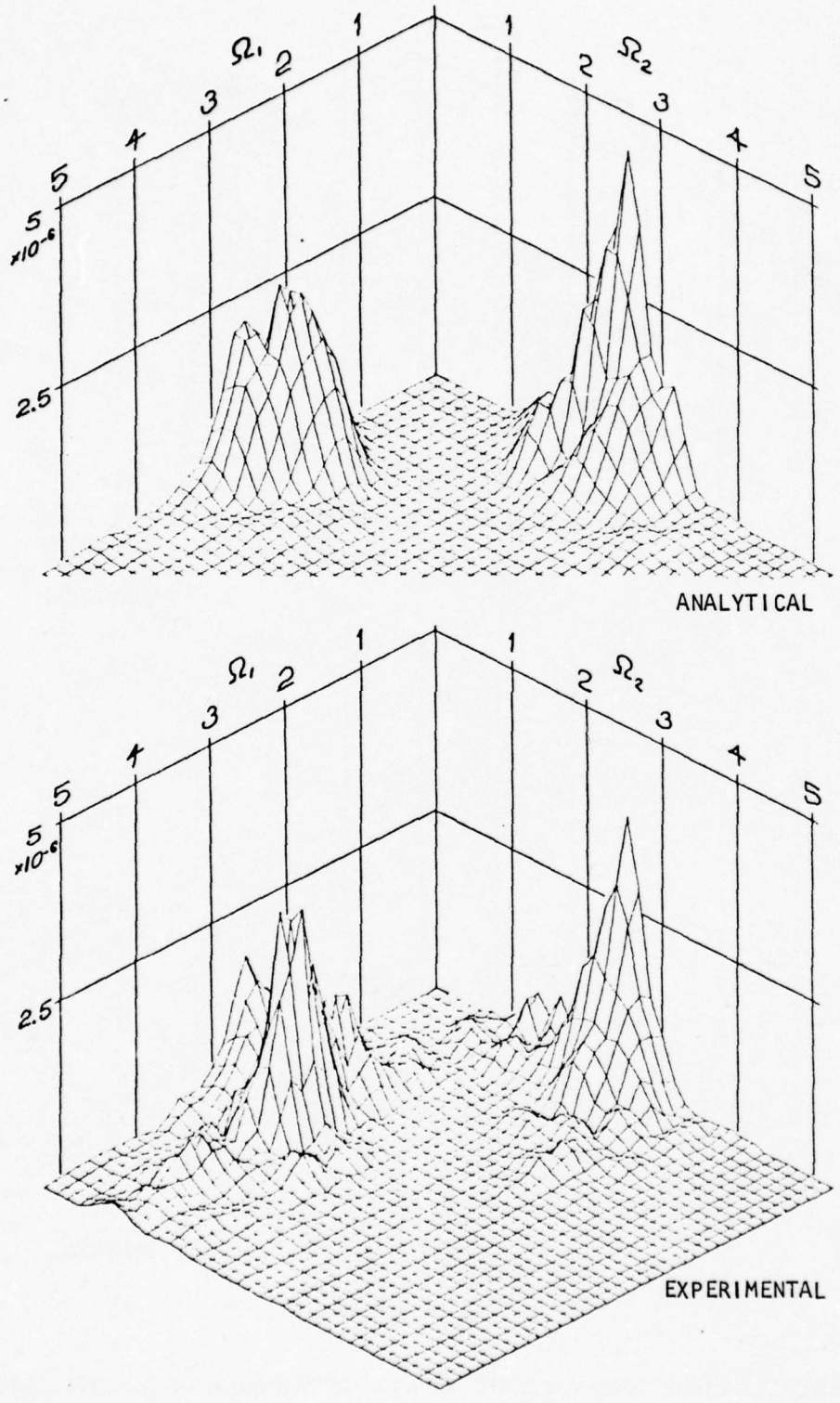

FIGURE 9 ANALYTICALLY PREDICTED AND EXPERIMENTALLY DERIVED CROSS-BI-SPECTRAL MODULI: FROUDE NUMBER 0.15, SEA STATE B

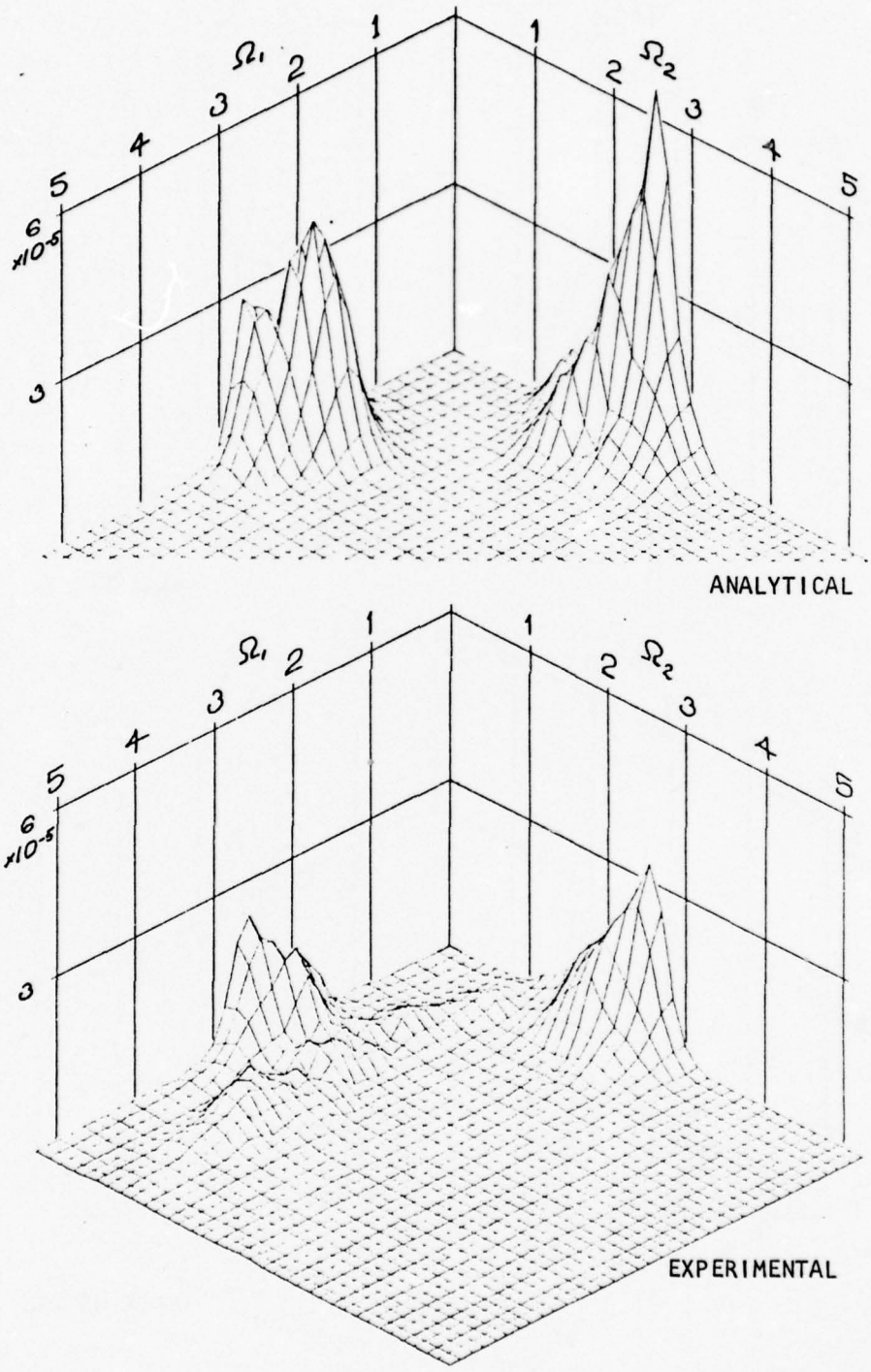

FIGURE 10 ANALYTICALLY PREDICTED AND EXPERIMENTALLY DERIVED CROSS-BI-SPECTRAL MODULI: FROUDE NUMBER 0.15, SEA STATE C

The triangular bi-frequency domain corresponds to that of Figure 6. At the bottom of each figure is the modulus of the experimental cross-bi-spectrum. Both parts of each figure are drawn to the same scale.

On the whole, in Figures 8 through 10, the major peaks which lie near the axes correlate fairly well. The largest such peaks are located at approximately the same sum or difference frequencies in both analytical and experimental results. The difference in magnitude is about 30% for Sea States A and B and for the peak located in the Ω_1 axis in Sea State C. The peaks along the sum frequency axis for Sea State C (Figure 10) are different by about a factor of 2. These margins of difference are roughly the same as that shown for the mean resistance operator in Figure 4.

A close comparison of the experimental results in Figures 8 through 10 discloses a range of humps lying along the line $\Omega_2 = 1$. The magnitude decreases as the sea severity increases. This characteristic is not present in the analytically derived cross-bi-spectra. There is in addition a significant hump along the line $\Omega_2 \approx 3.2$ in Figure 8 for Sea State A. This last corresponds to the contributions of a noise frequency which, as indicated in Ref. 1, has little to do with added resistance.

Overall, Figures 8 through 10 indicated a fair correlation between analysis and experiment, and that a more detailed comparison of real and imaginary parts of the quadratic frequency response functions would be worth-while.

The details of both real and imaginary parts of the analytical quadratic frequency response function are shown in comparison with the experimental results from Refs. 1 and 5 in Figures 11 through 16. In figures 11 and 12 the real and imaginary parts of the analytical result are compared with experimental results derived from model Sea State A, Figures 13 and 14 contain the corresponding comparison with results from model Sea State B, and Figures 15 and 16 involve the comparison with results from Sea State C.

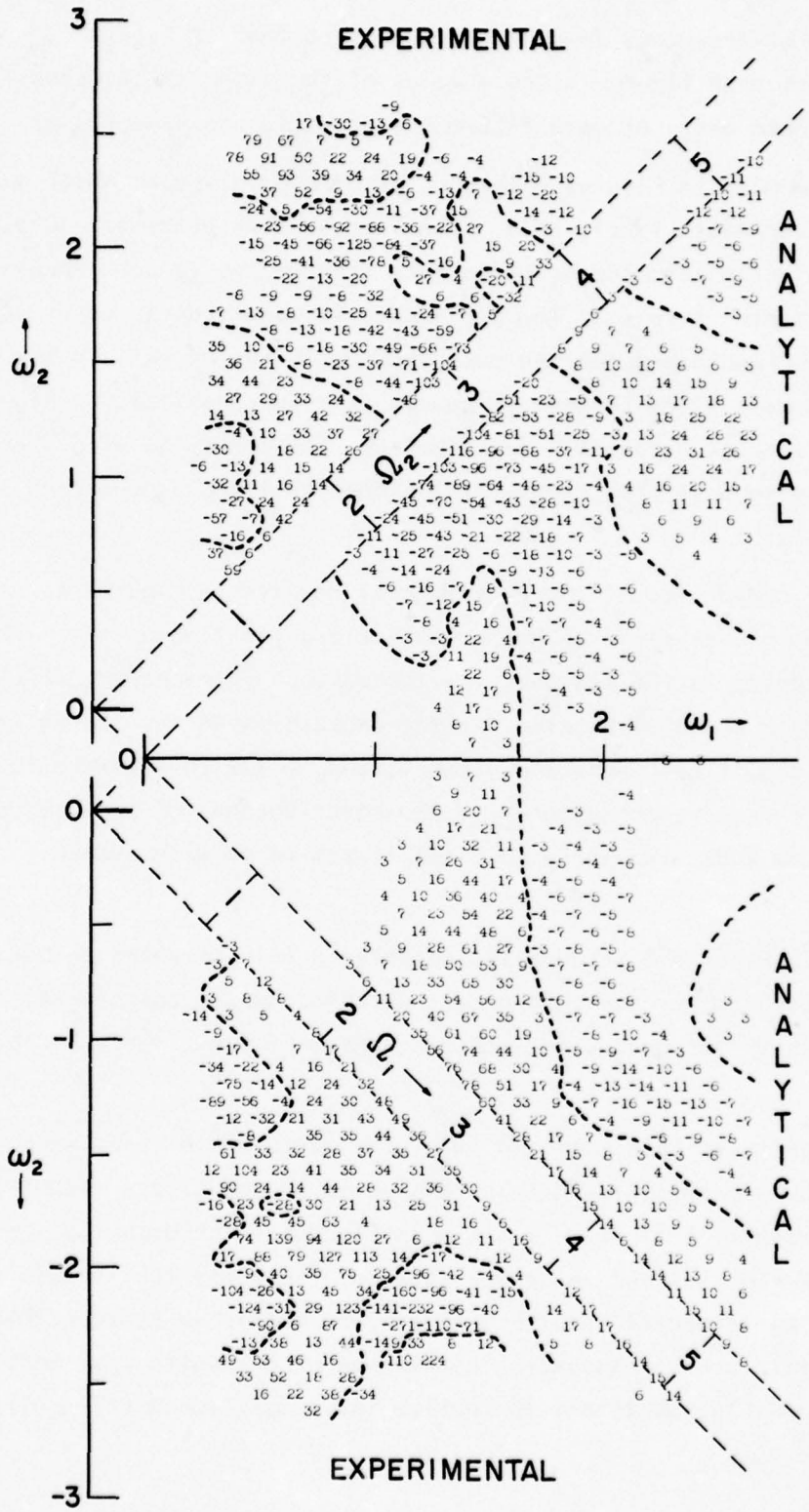

FIGURE 11 COMPARISON OF REAL PART OF ANALYTICAL QUADRATIC FREQUENCY RESPONSE FUNCTION WITH RESULTS FROM EXPERIMENT IN SEA STATE A, $F_n = 0.15$

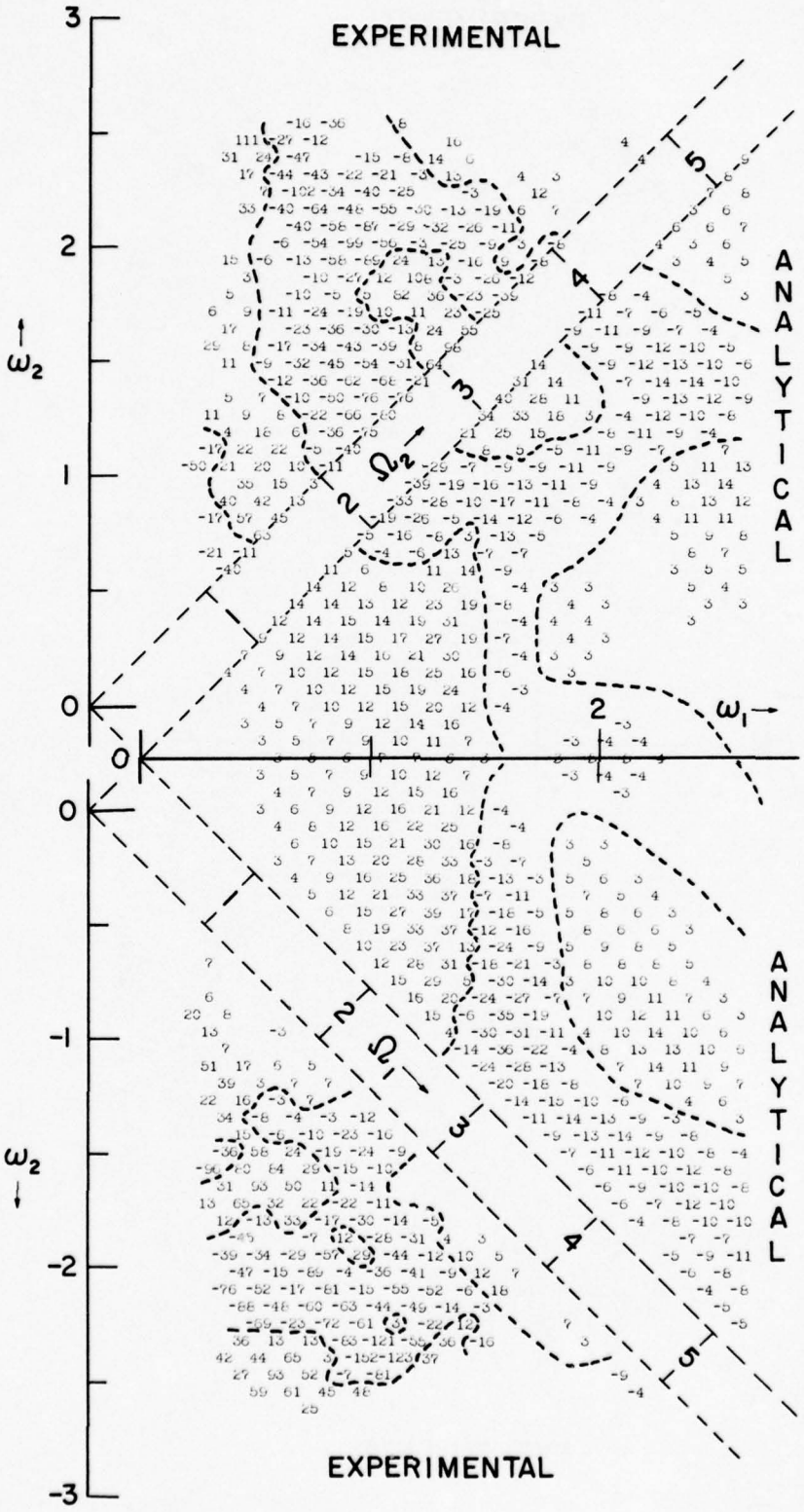

FIGURE 12 COMPARISON OF IMAGINARY PART OF ANALYTICAL QUADRATIC FREQUENCY RESPONSE FUNCTION WITH RESULTS FROM EXPERIMENT IN SEA STATE A, $F_n = 0.15$

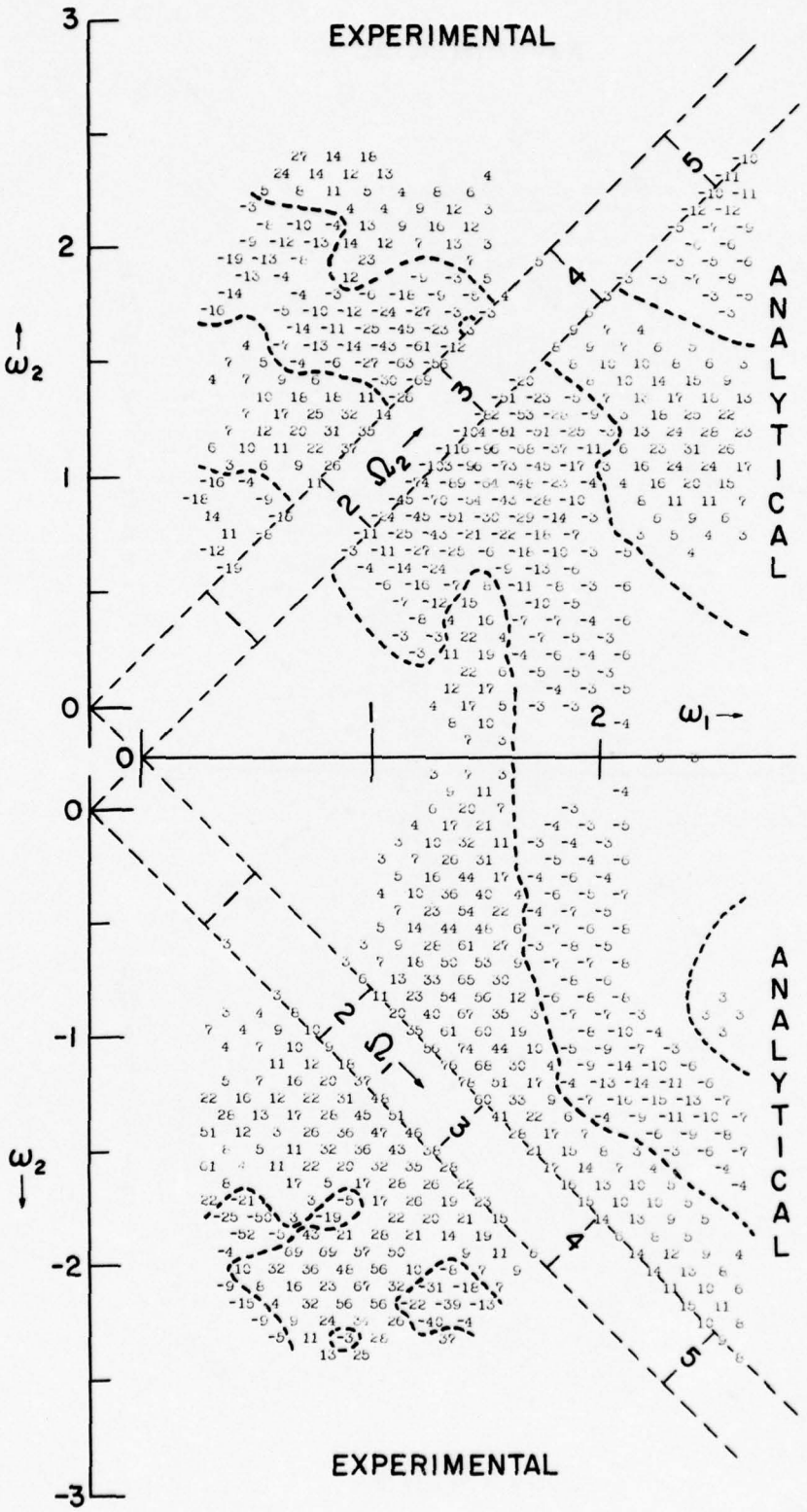

FIGURE 13 COMPARISON OF REAL PART OF ANALYTICAL QUADRATIC FREQUENCY RESPONSE FUNCTION WITH RESULTS FROM EXPERIMENT IN SEA STATE B, $F_n = 0.15$

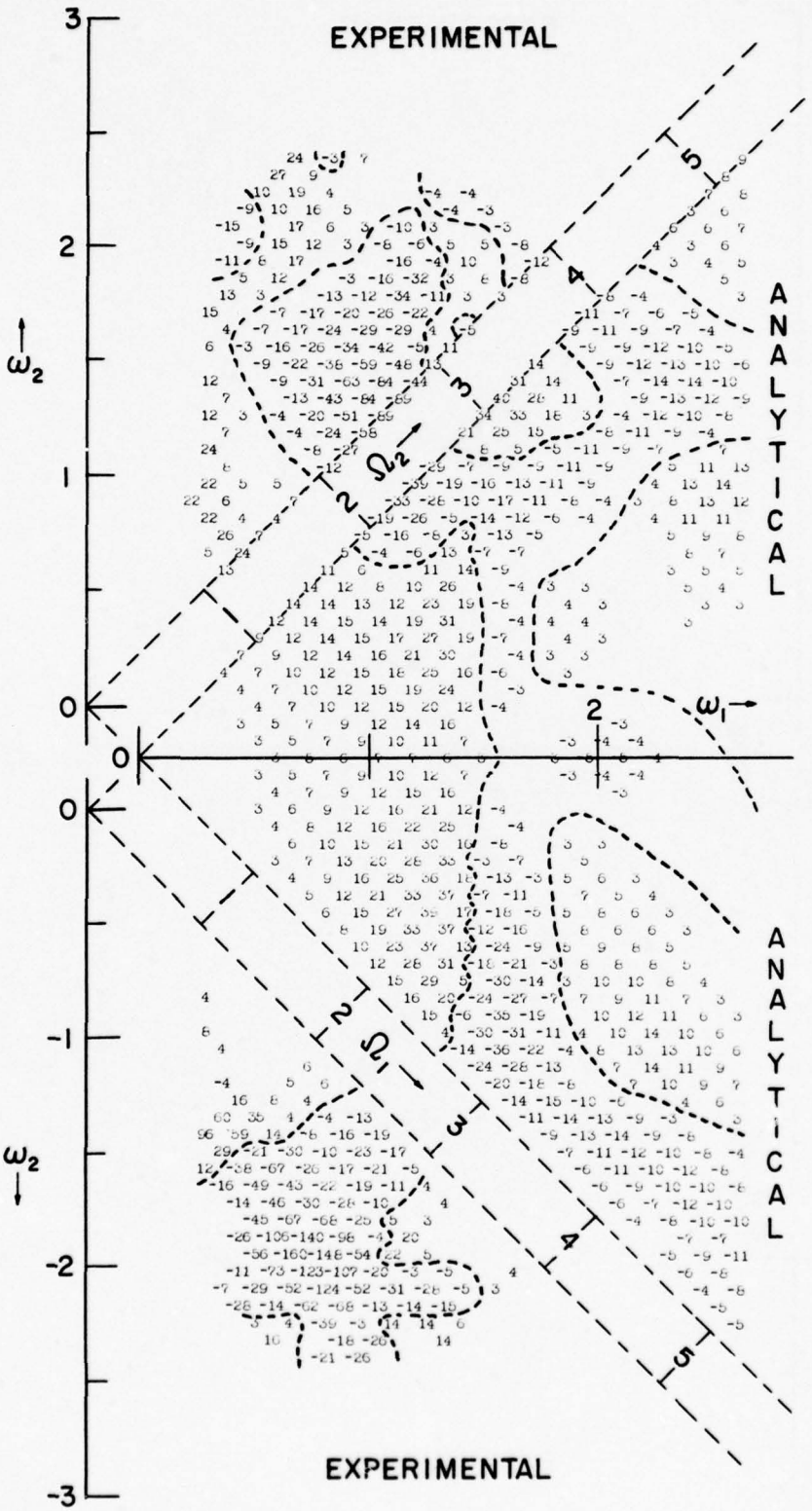

FIGURE 14 COMPARISON OF IMAGINARY PART OF ANALYTICAL QUADRATIC FREQUENCY RESPONSE FUNCTION WITH RESULTS FROM EXPERIM ENT IN SEA STATE B, $F_n = 0.15$

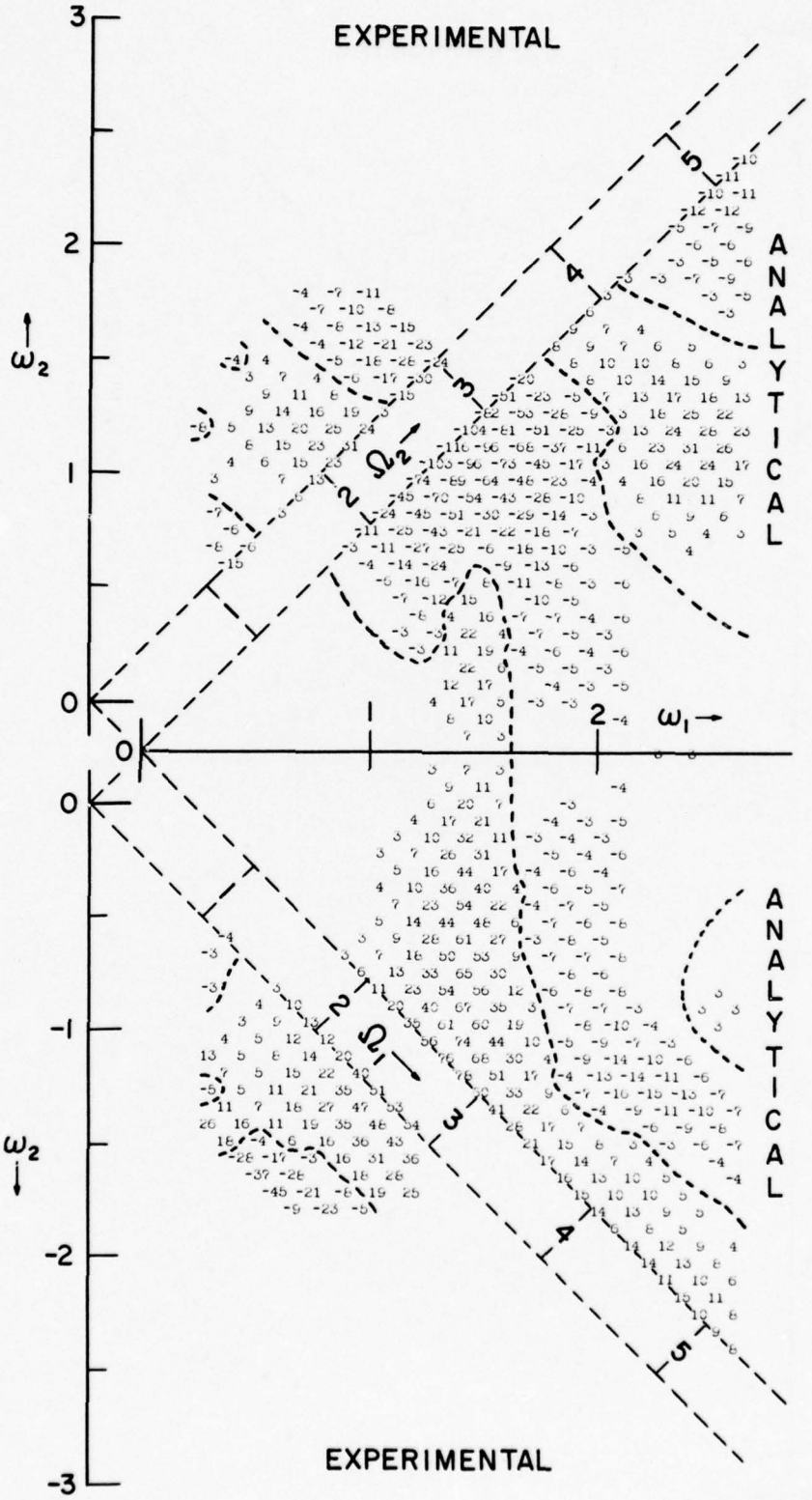

FIGURE 15 COMPARISON OF REAL PART OF ANALYTICAL QUADRATIC FREQUENCY RESPONSE FUNCTION WITH RESULTS FROM EXPERIMENT IN SEA STATE C, $F_n = 0.15$

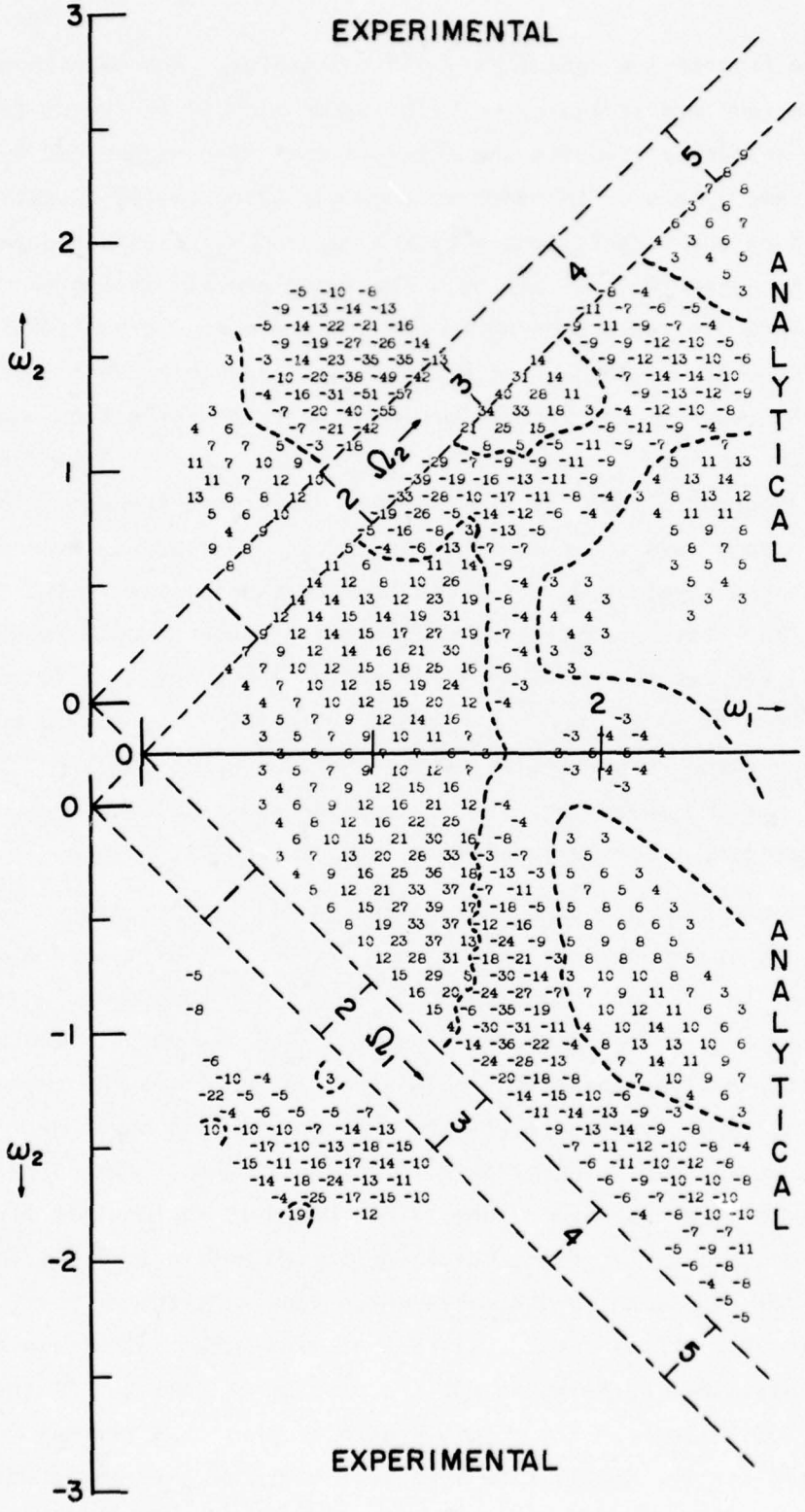

FIGURE 16 COMPARISON OF IMAGINARY PART OF ANALYTICAL QUADRATIC FREQUENCY RESPONSE FUNCTION WITH RESULTS FROM EXPERIMENT IN SEA STATE C, $F_n = 0.15$

These figures are essentially plotted tables. The magnitude of the function involved is indicated by a number plotted in the bi-frequency plane. The analytical results are shown in the quadrant bounded by the positive Ω_1 and Ω_2 axes. In order to show the experimental results in the same figure the octant bounded by the $+\omega_2$ and $+\Omega_2$ axes has been displaced in the negative Ω_1 direction. The experimental results shown in this octant are plotted according to the basic symmetry property of the quadratic frequency response. If analysis and experiment were in exact agreement the experimental results would be an exact reflection about the Ω_2 axis of the analytical results in the Ω_2 - ω_1 octant. A similar procedure was adopted to show the experimental difference frequency interactions. In this case the octant bounded by the $+\Omega_1$ and $-\omega_2$ axes is displaced in the negative Ω_2 direction and the experimental values are plotted so that exact analytical/experimental agreement would require the experimental results to be an exact reflection about the Ω_1 axis of the analytical results in the ω_1 - Ω_1 octant. (In this case strict compliance with the symmetry properties of the function would require that the sign of the imaginary part of the experimental result be changed. In order that comparison be made easier this has <u>not</u> been done.)

There are several other conventions in Figures 11 through 16. All magnitudes are rounded to the nearest integer. Analytical results were obtained for all positions in the Ω_2 - Ω_1 quadrant up to $\omega_1 = 2.62$. However, when a numerical result was between -2.5 and +2.5 it was omitted from the plot -- blank spaces in the analytical result may be taken to mean that the result was small. There are two possible meanings to blank space in the experimental portion of the figures. The first is the same as for the analytical case. The second is responsible for the concentration of experimental results in limited portions of the octants. It is that all experimental estimates which resulted from a wave,wave,$(\text{wave})^2$ cross-bi-spectral estimate less than 10% of its peak value were discarded as being of dubious statistical merit. (Actually there were indications in the previous work[1,5] that this truncation level is optimistic for the sample size involved -- 25% of peak could well have been a better choice.) The contours shown in the figures are for the zero level.

The results may be conveniently discussed according to bands of output frequency, Ω_2. The first band of frequency to be considered is that above $\Omega_2 \approx 3$. In this band the magnitude of the analytical result generally decreases from its peak along the Ω_2 axis to a minor hump centered at approximately $\Omega_2 = 4$, $\Omega_1 = 1$. Experimental results in this band are shown only for Sea States A and B, Figures 11 through 14, and the analyses of Ref. 1 indicated that much of the content of this band was related to towing system induced longitudinal vibration of the model. Thus agreement between analysis and experiment in the region above $\Omega_2 = 3$ was not expected. Despite this, there is a surprising resemblence in the position of the zero level contours. The real part of the functions are negative at $\Omega_2 = 3$, make a transition to positive halfway between $\Omega_2 = 3$ and 4 and then tend to return to negative after $\Omega_2 = 4$. The correspondence in zero contour position in the imaginary parts, Figures 12 and 14, is as good, a small positive area appears centered on $\Omega_2 = 3.25$ and this is surrounded by negatives. Agreement in magnitudes of real and imaginary parts in this band is best in Figures 13 and 14 for Sea State B where the influence of vibration on experiments was not so large. The corresponding comparison in Figures 11 and 12 for Sea State A shows large differences in magnitude.

The fact that apparently un-correlated noise appeared to influence the cross-bi-spectral estimates of response could not be explained in Ref. 1. The similarity in the behavior of the analytical and experimental results gives rise to the speculation that the problem vibration of Refs. 1 and 5 might have been induced at least partially by the quadratic component of the wave exciting force and not by mechanical imperfections in rail and equipment as was supposed.

The next band of output frequency which may be considered is that between $\Omega_2 = 2$ and 3. This is the band where the experimental estimates were considered most significant. The level of agreement between the moduli of analytical and experimental results has previously been noted in connection with Figures 8-10. The position of zero contours in the imaginary part of all experimental estimates correlates quite well with the analytical (Figs.12,14 and 16). However in the real parts of the

experimental estimates (Figs.11,13,15) the zero contour is consistently midway between the limits of the band while the analytical result is almost all negative. Here there is a clear inconsistency between experiment and analysis. The fair agreement in moduli suggests that the phase reference correction to the experimental data somehow does not reflect the actual conditions of experiment, or that the radical "hook" in the analytical zero contour in the region $\Omega_2 = 2$, $\Omega_1 = 1$ should not be present. Neither supposition can be proven at present.

The experimental results from Sea States A and B (Figs.11-14) which are shown for Ω_2 less than 2 in the upper octant correlate badly with the analytical result. Only in the case of the imaginary part derived from Sea State C (Fig.16) is there reasonably good correlation. The experimental estimates in this region were derived from wave,wave,resistance cross-bi-spectral estimates of relatively low magnitude, and it appears that the analytical result bears out the supposition made in Ref. 1 that the experimental results in this region tend to suffer from sampling variability.

The first band of output frequency to be discussed in the lower octant is that from $\Omega_2 = 0$ to 0.5. For practical purposes the correlation of real parts in this band has been shown in Figure 4. The correlation of imaginary parts in this band may be regarded as fair, considering that the imaginary part of the function is relatively low and that the experimental results are sparse in some cases.

The last band of output frequency in the lower octant to be discussed is that between $\Omega_2 = 0.5$ and 1.5. This is an interesting band in that response originating in quadratic interactions is combined with linear response at frequencies important to ship motions. The analytical results show a significant interaction response in the neighborhood of $\Omega_2 = 1$, $\Omega_1 = 2$. The experimental results from Sea State B (Figs.13,14) come closest to suggesting the same interaction, those from Sea State C (Figs.15,16) are too sparse for comparison, but those from Sea State A agree rather badly. The validity of some of these experimental results was questioned in Ref. 1 since they also were derived from relatively low values of wave,wave,resistance cross-bi-spectra.

In the remainder of the Ω_2 = 0.5 to 1.5 band a significant response in the region near Ω_1 = 3 could not be questioned in Ref. 1. There is clearly no correlation with the analytical result in this case. The very significant interaction result near Ω_1 = 4 which was obtained by reduction of data from Sea State A (Figs.11,12) was questioned on sampling variability grounds in Ref. 1, and it is clear from the analytical result that this interaction cannot be substantiated.

SUMMARY

The general objective of the present work was to make an extension to existing hydrodynamic theory for ship resistance added by waves, to include time dependent fluctuations so that the quadratic frequency response function for added resistance could be computed. It was clear that work of this nature might provide considerable insight into the nature of resistance fluctuations in random seas, and, by providing a physical model, clarify previously obtained experimental estimates of the function.

Given the definition and interpretation of the quadratic frequency response function which is afforded by the functional polynomial input-output model, as well as an existing generalized expression for hydrodynamic force on a body in potential flow, the general formulation of the hydrodynamic problem was found to be straightforward within the constraints of one cardinal assumption. This assumption is that the dominant contribution to second order non-linear force response is due to the products of first order potentials which arise from the Bernoulli Equation -- and not from nonlinearities in the potentials themselves. The resulting general formulation is not limited to added resistance, and may have application in other problems.

The evaluation of the quadratic frequency response function for added resistance was carried out according to a strip method in which the sectional wave diffraction induced forces as well as forces induced by body motion were evaluated by close fit methods. Because the mean added resistance operator, which is generally the only result from other analytical methods, is a special part of the quadratic response function it was possible to compare the results of the present method with some other analytical results and with results from the usual added resistance experiment. The present analytical method appears valid on this basis, and in fact appears to have promise as an improvement in the analytical computation of mean added resistance.

In the previous experimental work three sets of estimates of the quadratic frequency response function for added resistance had been made for each of two model speeds of a Series 60 0.60 block model by means of cross-bi-spectral analysis of data obtained in irregular waves. Because the wave severity had been varied over a good part of the range of practical interest, an approximate equivalence of the main features of the quadratic frequency response functions derived from data obtained in different sea states was taken to mean that the concept of a quadratic frequency response function was viable. There were necessarily statistical complications entering into the data reduction process so that those experimental estimates which were considered to be at least tentatively valid did not cover the entire bi-frequency domain of interest, and were not themselves all of the same reliability.

The present analytical methods were utilized to compute the complete function for one of the conditions of the experiments, and these results were compared with experiment in several ways. In the quantitative sense, the correlation between analytical and experimental frequency response functions may be considered fair, at least for the predominant features. In this context it should be remarked that the correlation between experimental and analytical results for the mean added resistance operator can also only be considered fair. Better quantitative correlation for the rest of the quadratic frequency response function can hardly be expected. Over all, there is at least a reasonable resemblence between experiment and analysis with respect to the contours of zero level in real and imaginary parts of the function; that is, with respect to phase. Analysis and experiment do not agree well in the band of the bi-frequency plane in which the interaction response is at frequencies coinciding with the range important for ship motions. Both sets of results imply a significant interaction response, but disagree about what combination of input frequencies are of most importance.

The most important concern in the present work was qualitative. The fundamental questions were: a) what is the nature and general behavior of the quadratic frequency response function outside the range of experimental data, and b) could the predominant features of the function as shown by experiment be confirmed?

There appears to be good qualitative agreement between analysis and experiment with respect to the most prominent features of the function. These prominent features involve a hump containing the peak values of the mean added resistance operator, and a hump of typically larger magnitude associated with sum-frequency and second harmonic response. Apart from these main features, the analytical results imply the existence of secondary humps in many of those regions of the bi-frequency plane which could not be covered by experiment. Most of the experimental estimates which were previously considered of marginal reliability were also not confirmed by the analytical results. Since it was these marginal experimental estimates which gave rise to the speculation that the quadratic frequency response function was inordinately complicated, the present work indicates that the function is merely a moderately complicated function of two frequencies.

Because the present results are thought to be the first of their kind, firm conclusions seem premature. It is apparent that confirmation of the actual level of accuracy of the analytical method must await experimental data containing fewer caveats. However the work demonstrates that it is feasible to make an at least approximately correct hydrodynamic estimate of the response function -- which in turn allows interpretation or prediction of non-linear fluctuations of resistance in a random seaway.

RECOMMENDATIONS

It appears that reasonable qualitative agreement has been achieved between experimental and analytical estimates of quadratic frequency response for added resistance. The natural next step might be to refine the computational methods so as to achieve better detailed agreement. In the present case however the only experimental estimates which were available may have been obtained in the hardest possible way -- that is by analysis of irregular wave experiments. This was a natural approach in demonstrating the applicability of the input-output model, but the results obtained substantiate the earlier fears that substantial uncertanties related to sample size exist. It is accordingly recommended that the most fruitful next step in the development would be to develop dual frequency experimental techniques (without statistical complications) which would produce results directly comparable to analysis.

The analytical methods utilized herein appear to have some promise in the sense of improving theoretical estimates of mean added resistance operators. Trial application of the method to a wider range of ship forms is recommended.

REFERENCES

1. Dalzell, J.F., "Application of the Functional Polynomial Model to the Ship Added Resistance Problem," Paper presented at the Eleventh Symposium on Naval Hydrodynamics, London, March 1976.

2. Dalzell, J.F., "Application of Cross-Bi-Spectral Analysis to Ship Resistance in Waves," SIT-DL-72-1606, AD749102, Davidson Laboratory, Stevens Institute of Technology, May 1972.

3. Dalzell, J.F., "Some Additional Studies of the Application of Cross-Bi-Spectral Analysis to Ship Resistance in Waves," SIT-DL-72-1641, AD757363, Davidson Laboratory, Stevens Institute of Technology, December 1972.

4. Dalzell, J.F., "Cross-BiSpectral Analysis: Application to Ship Resistance in Waves," Journal of Ship Research, Vol. 18, No. 1, March 1974, pp 62-72.

5. Dalzell, J.F., "The Applicability of the Functional Polynomial Input-Output Model to Ship Resistance in Waves," SIT-DL-75-1794, Davidson Laboratory, Stevens Institute of Technology, January 1975.

6. Salvesen, N., "Second-Order Steady-State Forces and Moments on Surface Ships in Oblique Regular Waves," Paper 22, International Symposium on Dynamics of Marine Vehicles and Structures in Waves, London, April 1974.

7. Kim, C.H., "Calculation of Motions and Loads of a Ship Uniformly Advancing in Oblique Regular Waves," Technical Memorandum SIT-DL-74-166, March 1974.

8. Kim, C.H. and Chou, F., "Wave-Exciting Forces and Moments on an Ocean Platform in Oblique Seas," Paper No. OTC 1180, Offshore Technology Conference, April 1970. Also SIT-OE-71-Report 6, September 1971.

9. Frank, W., "On the Oscillation of Cylinders in or Below the Free Surface of Deep Fluids," NSRDC Report 2375, October 1967.

10. Strom-Tejsen, J., Yeh, H.Y.H., and Moran, D.C., "Added Resistance in Waves," SNAME Vol. 81, pp 109, 1973.

APPENDIX A

DIFFRACTION FORCES AND MOMENTS ON A UNIFORMLY TOWED RESTRAINED SHIP IN OBLIQUE WAVES

1. A Brief Description of the Method for Zero Speed[8]

The problem is to formulate the wave-exciting forces and moments on a fixed ship in oblique regular waves.

Set the right-handed fixed coordinate system X,Y,Z on the ocean's surface. Precisely, the X-Y plane rests on the calm water surface (see Figure 2). An incident wave which progresses across the X-axis obliquely at angle μ with the X-axis is

$$h = a\, e^{i(\nu_o X\cos\mu + \nu_o Y\sin\mu - \omega_o t)} \tag{A-1}$$

where

a = wave amplitude

ω_o = circular wave frequency

ν_o = wave number ($= \omega_o^2/g$)

The velocity potential which generates the wave h is expressed in the form

$$\Phi_I(X,Y,Z;\ \nu_o,\mu;t) = \varphi_I(Y,Z;\nu_o,\mu)\, e^{i(\nu_o X\cos\mu - \omega_o t)} \tag{A-2}$$

where

$$\varphi_I(Y,Z;\nu_o,\mu) = -\frac{iga}{\omega_o}\, e^{\nu_o Z}\ e^{i\nu_o Y\sin\mu} \tag{A-3}$$

The diffraction potential is regarded as the direct response to the incident wave potential. In view of this fact, we assume the diffraction potential Φ_D to be similar in form to Φ_I, as follows:

$$\Phi_D(X,Y,Z;\nu_o,\mu;t) = \varphi_D(Y,Z;\nu_o,\mu)\, e^{i(\nu_o X\cos\mu - \omega_o t)} \tag{A-4}$$

where

$$\varphi_D(Y,Z;\nu_o,\mu) = \int_{C(x)} Q(\eta,\zeta)\, G(Y,Z;\eta,\zeta;\nu_o)\, dC \qquad (A-5)$$

In the above, the Green function G is the two-dimensional pulsating source potential of unit intensity at the point (η,ζ) in the lower half of the Y-Z plane.[9] $C(x)$ indicates that the integral is to be taken along a hull-section contour below the calm water surface. The unknown source intensities Q which are discretely distributed along the contour $C(x)$ are determined by satisfying the condition of non-penetration of the water particles across the contour. This kinematical boundary condition is

$$\frac{\partial \varphi_D}{\partial n} = - \frac{\partial \varphi_I}{\partial n} \qquad \text{on } C(x) \qquad (A-6)$$

The diffraction potential satisfies

1. the continuity condition
2. the linearized free surface condition
3. the radiation condition
4. the deep water condition

2. Extension of the Previous Method to the Non-Zero Speed Case

In dealing with the diffraction of waves due to a uniformly moving ship, it is required to introduce the moving coordinate system x,y,z which coincides with the fixed system X,Y,Z at time $t=0$ and moves along the X-axis at speed U (see Figure 2). The transformation of the coordinate system is then given by

$$\begin{aligned} X &= x + Ut \\ Y &= y \\ Z &= z \end{aligned} \qquad (A-7)$$

whereas the frequency of encounter ω is

$$\omega = \omega_o - U\, \nu_o \cos\mu \qquad (A-8)$$

with

ω_o = the wave frequency

ν_o = the wave number ω_o^2/g

The incident wave and its corresponding velocity potential in the fixed coordinate system, Eqs.(A-1, A-2, A-3), are transformed by substituting Eqs.(A-7) and (A-8). Thus,

$$h = a\, e^{i(\nu_o x\cos\mu + \nu_o y\sin\mu - \omega t)} \tag{A-9}$$

$$\Phi_I(x,y,z;\nu_o,\mu;t) = \varphi_I(y,z;\nu_o,\mu)\, e^{i(\nu_o x\cos\mu - \omega t)} \tag{A-10}$$

with

$$\varphi_I(y,z;\nu_o,\mu) = -\frac{iga}{\omega_o}\, e^{\nu_o z}\, e^{i\nu_o y\sin\mu} \tag{A-11}$$

It might seem that the diffraction potential which is regarded as the response to the incident wave potential(A-10) should assume an expression similar to that given in(A-4). However, then the convective term $U\frac{\partial}{\partial x}$ would vanish. The time derivative $\frac{\partial}{\partial t}$ of the diffraction potential with respect to the fixed frame is now replaced by the sum of local and convective terms $\frac{\partial}{\partial t} - U\frac{\partial}{\partial x}$ with respect to the moving frame. For instance, the linearized free surface condition is

$$\left[\left(\frac{\partial}{\partial t} - U\frac{\partial}{\partial x}\right)^2 + g\frac{\partial}{\partial z}\right]\Phi_D(x,y,z;\nu,\mu;t) = 0 \qquad \text{on } z=0 \tag{A-12}$$

In view of the above remarks, we assume that

$$\Phi_D(x,y,z;\nu,\mu;t) = \varphi_D(x,y,z;\nu,\mu)\, e^{i(\nu_o x\cos\mu - \omega t)} \tag{A-13}$$

where

$$\varphi_D(x,y,z;\nu,\mu) = \varphi_D^*(y,z;\nu,\mu) \qquad \text{on } C(x)\ , \tag{A-14}$$

$$\varphi_D^* = \int_{C(x)} Q(\eta,\zeta)\, G(y,z;\eta,\zeta;\nu)\, dC\ , \tag{A-14a}$$

$$\nu = \omega^2/g\ ,$$

and φ_D^* varies as the form of the hull section varies along the hull length. The above assumption paves the way for the stripwise calculation to be carried out in a rational manner.

The kinematical boundary condition for the potential $\varphi_D+\varphi_I$ is

$$\frac{\partial\varphi_D^*(y,z;\nu,\mu)}{\partial n} = -\frac{\partial\varphi_I(y,z;\nu_o,\mu)}{\partial n} \qquad \text{on } C(x) \tag{A-15}$$

The procedure for satisfying the kinematical boundary condition follows.

First, define the odd and even function of φ_I in Eq. (A-11):

$$\varphi_I^{(o)} = \frac{ga}{\omega_o} e^{\nu_o z} \sin(\nu_o y \sin\mu)$$

$$\varphi_I^{(e)} = \frac{ga}{\omega_o} e^{\nu_o z} \cos(\nu_o y \sin\mu) \tag{A-16}$$

The normal derivatives of $\varphi_I^{(o)}$ and $\varphi_I^{(e)}$ are given by

$$\frac{1}{a}\frac{\partial\varphi_I^{(e)}}{\partial n} = -\omega_o e^{\nu_o z}[\sin\mu\sin(\nu_o y\sin\mu)\sin\alpha+\cos(\nu_o y\sin\mu)\cos\alpha]$$

$$\frac{1}{a}\frac{\partial\varphi_I^{(o)}}{\partial n} = \omega_o e^{\nu_o z}[\sin\mu\cos(\nu_o y\sin\mu)\sin\alpha-\sin(\nu_o y\sin\mu)\cos\alpha] \tag{A-17}$$

where α is the slope of the contour $C(x)$ at a point (y,z).

On substituting (A-14) and (A-17) in (A-15), we have for the sway-exciting force

$$\sum_{j=1}^{N} Q_j^{(2)} I_{ij}^{(2)} + \sum_{j=1}^{N} Q_{N+j}^{(2)} J_{ij}^{(2)} = -\omega_o e^{\nu_o z_i}[\sin\mu\cos(\nu_o y_i\sin\mu)\sin\alpha_i - \sin(\nu_o y_i\sin\mu)\cos\alpha_i]$$

$$-\sum_{j=1}^{N} Q_j^{(2)} J_{ij}^{(2)} + \sum_{j=1}^{N} Q_{N+j}^{(2)} I_{ij}^{(2)} = 0 \tag{A-18}$$

and for the heave-exciting force

$$\sum_{j=1}^{N} Q_j^{(3)} I_{ij}^{(3)} + \sum_{j=1}^{N} Q_{N+j}^{(3)} J_{ij}^{(3)} = 0$$

$$-\sum_{j=1}^{N} Q_j^{(3)} J_{ij}^{(3)} + \sum_{j=1}^{N} Q_{N+j}^{(3)} I_{ij}^{(3)} = -\omega_o e^{\nu_o z_i} [\sin\mu \sin(\nu_o y_i \sin\mu) \sin\alpha_i + \cos(\nu_o y_i \sin\mu) \cos\alpha_i] \qquad \text{(A-19)}$$

where $I_{ij}^{[m]}$ and $J_{ij}^{[m]}$ are the "influence coefficients" given in the Appendix of Reference 9. For roll, the formula is the same as for sway, except that the mode number is 4 instead of 2.

If N sources are taken (i.e., i=1,2,... N), we obtain a $[2N]\cdot[2N]$ system of equations with 2N unknowns, giving the real and imaginary parts of the unknown complex source intensities Q.

Solutions of (A-18) and (A-19) yield the diffraction potentials $\varphi_D^{*(o)}$ and $\varphi_D^{*(e)}$ for a strip section contour $C(x)$.

The diffraction-induced hydrodynamic pressure at a point on the hull surface, for instance, for the even function which contributes to the heaving force, is

$$p = \left[i\omega\rho + \rho U \frac{\partial}{\partial x} \right] \varphi_D^{(e)}(x,y,z;\nu,\mu) e^{i\nu_o x \cos\mu} \qquad \text{(A-20)}$$

where the time factor $e^{-i\omega t}$ is omitted.

The integration of the vertical components of the above pressure first along the contour $C(x)$ and second along the hull length between $-\ell_1$ and ℓ_2 yields the diffraction-induced heave-exciting force in the form

$$\frac{F_{\zeta h}^{D}}{a} = \left(1 + \frac{U\nu_o \cos\mu}{\omega}\right) \int_{-\ell_1}^{\ell_2} e^{i\nu_o x \cos\mu} dx \int_{C(x)} i\rho\omega\varphi_D^{(e)}(x,y,z;\nu,\mu) dy$$

$$+ \frac{U}{i\omega} \int_{-\ell_1}^{\ell_2} e^{i\nu_o x \cos\mu} dx \frac{d}{dx} \int_{C(x)} i\rho\omega\varphi_D^{(e)}(x,y,z;\nu,\mu) dy \qquad \text{(A-21)}$$

The relation

$$\frac{d}{dx}\int_{C(x)} i\rho\omega\varphi_D^{(e)}(x,y,z;\nu,\mu)\,dy = \int_{C(x)} i\rho\omega\,\frac{\partial}{\partial x}\,\varphi_D^{(e)}(x,y,z;\nu,\mu)\,dy \qquad (A\text{-}22)$$

has been used in the foregoing derivation.

In carrying out the integral along the contour $C(x)$ in Eq.(A-21), we make use of the relation (A-14) for $\varphi_D^{*}(y,z;\nu,\mu)$ and designate the integral by $f_H^D(x)$,

$$f_H^D(x) = \int_{C(x)} i\rho\omega\varphi_D^{*(e)}(y,z;\nu,\mu)\,dy \qquad (A\text{-}23)$$

Now the integration of (A-21) by parts with respect to x yields

$$\frac{F_{\zeta h}^D}{a} = \int_{-\ell_1}^{\ell_2} e^{i\nu_o x\cos\mu} f_H^D(x)\,dx - \frac{U}{i\omega} f_H^D(-\ell_1)e^{-i\nu_o\ell_1\cos\mu} \qquad (A\text{-}24)$$

where

$f_H^D(-\ell_1)$ is Eq.(A-23) for $x = -\ell_1$.

The diffraction-induced sway- and roll-exciting forces and moments are evaluated in similar fashion:

$$\frac{F_{\eta h}^D}{a} = \int_{-\ell_1}^{\ell_2} e^{i\nu_o x\cos\mu} f_S^D(x)\,dx - \frac{U}{i\omega} f_S^D(-\ell_1)e^{-i\nu_o\ell_1\cos\mu} \qquad (A\text{-}25)$$

$$\frac{F_{\varphi h}^D}{a} = \int_{-\ell_1}^{\ell_2} e^{i\nu_o x\cos\mu} f_R^D(x)\,dx - \frac{U}{i\omega} f_R^D(-\ell_1)e^{-i\nu_o\ell_1\cos\mu} \qquad (A\text{-}26)$$

where

$$f_S^D(x) = -\int_{C(x)} i\rho\omega\varphi_D^{*(o)}\,dz \qquad (A\text{-}27)$$

$$f_R^D(x) = \int_{C(x)} i\rho\omega\varphi_D^{*(o)}\,(ydy + zdz) \qquad (A\text{-}28)$$

A similar procedure is also applied to calculate the pitch- and yaw-exciting moments. For example, the pitch-exciting moment is

$$\frac{F^D_{\psi h}}{a} = -\left(1 + \frac{U\nu_o \cos\mu}{\omega}\right) \int_{-\ell_1}^{\ell_2} e^{i\nu_o x\cos\mu}\, x\,dx \int_{C(x)} i\rho\omega\varphi_D^{(e)}\, dy$$

$$- \frac{U}{i\omega} \int_{-\ell_1}^{\ell_2} e^{i\nu_o x\cos\mu}\, x\,dx \frac{d}{dx} \int_{C(x)} i\rho\omega\varphi_D^{(e)}\, dy \qquad \text{(A-29)}$$

On substituting $f^D_H(x)$ of Eq.(A-23) into the above equation and integrating by parts in the second integral, we have

$$\frac{F^D_{\psi h}}{a} = -\int_{-\ell_1}^{\ell_2} x\, d\, e^{i\nu_o x\cos\mu}\, f^D_H(x)\,dx + \frac{U}{i\omega} \int_{-\ell_1}^{\ell_2} e^{i\nu_o x\cos\mu} f^D_H(x)\,dx$$

$$- \frac{U\ell_1}{i\omega} f^D_H(-\ell_1) e^{-i\nu_o \ell_1 \cos\mu} \qquad \text{(A-30)}$$

The yaw-exciting moment is obtained as

$$\frac{F^D_{Xh}}{a} = \int_{-\ell_1}^{\ell_2} x\, e^{i\nu_o x\cos\mu}\, f^D_S(x)\,dx - \frac{U}{i\omega} \int_{-\ell_1}^{\ell_2} e^{i\nu_o x\cos\mu} f^D_S(x)\,dx$$

$$+ \frac{U\ell_1}{i\omega} f^D_S(-\ell_1) e^{-i\nu_o \ell_1 \cos\mu} \qquad \text{(A-31)}$$

PRINCIPAL NOTATION

a_i	amplitude of wave component of frequency ω_i
B	beam of a section in the load waterplane
C(x)	a transverse section contour
$D_w(t)$	resistance added by waves
$\vec{F}$	hydrodynamic force
F_n	Froude Number
$f_H^D(\omega_i)$	sectional heave diffraction force per unit wave amplitude
$G_1(\omega)$	linear frequency response function
$G_2(\omega_1, \omega_2)$	quadratic frequency response function
$g_1(t)$	linear impulse response
$g_2(t_1, t_2)$	second degree kernel analogous to an impulse response
$H_1(\omega_i, \omega_j)$, $H_1(\omega_i, -\omega_j)$	functions defined by Eqs. (20) and (21)
$H_2(\omega_i, \omega_j)$, $H_2(\omega_i, -\omega_j)$	functions defined by Eqs. (22) and (23)
L	hull length
$m''(\omega_i)$	sectional heave added mass
$N(\omega_i)$	sectional damping coefficient
n	outward unit normal vector
$\underline{n}$	the z-component of the unit normal on the hull surface
$\vec{R}$	quadratic part of the added resistance

$\vec{R}_2$	force due to two superimposed regular wave trains
S_B	submerged surface of the body
S_F	portion of the free surface inside a far field control surface, S_∞
$\bar{T}$	average section draft
t	time
U	ship speed
$V^{(m)}(\omega_i)$	velocity amplitude of heave (m=3) and pitch (m=5)
X,Y,Z	fixed coordinates
x,y,z	moving coordinates
Δ	model displacement
ζ	heave amplitude
ζ_i	wave elevation of the i^{th} wave train
$\eta(t)$	wave elevation
ν_{o_i}	wave number corresponding to i^{th} wave train
ρ	mass density
Φ	total velocity potential
Φ_B	body potential
Φ_I	incident wave potential
Φ_S	wave resistance potential, steady state
Φ_T	time dependent potential due to waves

$\varphi_B(\omega_k)\,\mathrm{Exp}[-i\omega_k t]$	body potential, encounter frequency ω_k
$\varphi_D(\omega_i)$	the diffraction potential per unit wave amplitude in the i^{th} wave train
$\varphi_I(\omega_k)\,\mathrm{Exp}[-i\omega_k t]$	incident wave potential, encounter frequency, ω_k
$\varphi^{(m)}(\omega_i)$	radiation potential due to heaving and pitching motions, each per unit velocity amplitude
ψ	pitch amplitude
Ω_1	difference frequency
Ω_2	sum frequency
$\omega, \omega_1, \omega_2$	frequency
ω_{o_i}	wave frequency corresponding to i^{th} wave train

DISTRIBUTION LIST
Contract N00014-76-C-0347

40 Commander
David W. Taylor Naval Ship
Research & Development Center
Bethesda, MD 20084
Attn: Code 1505 (1)
Code 5211.4 (39 cys)

1 Officer-in-Charge
Annapolis Laboratory
Naval Ship Research and
Development Center
Annapolis, MD 21402
Attn: Code 522.3 (Library)

7 Commander
Naval Sea Systems Command
Washington, DC 20360
Attn: SEA 09G32 (3 cys)
SEA 03512 (Peirce) (1)
SEA 037 (1)
SEA 0322 (1)
SEA 033 (1)

12 Director
Defense Documentation Center
5010 Duke Street
Alexandria, VA 22314

1 Office of Naval Research
800 N. Quincy Street
Arlington, VA 22217
Attn: Mr. R.D. Cooper (Code 438)

1 Office of Naval Research
Branch Office
492 Summer Street
Boston, MA 02210

1 Office of Naval Research
Branch Office (493)
536 S. Clark Street
Chicago, IL 60605

1 Chief Scientist
Office of Naval Research
Branch Office
1030 E. Green Street
Pasadena, CA 91106

1 Office of Naval Research
Resident Representative
715 Broadway (5th Floor)
New York, NY 10003

1 Office of Naval Research
San Francisco Area Office
760 Market Street, Rm 447
San Francisco, CA 94102

2 Director
Naval Research Laboratory
Washington, DC 20390
Attn: Code 2027 (1)
Code 2629 (ONRL) (1)

1 Commander
Naval Facilities Engineering
Command (Code 032C)
Washington, DC 20390

1 Library of Congress
Science & Technology Division
Washington, DC 20540

8 Commander
Naval Ship Engineering Center
Center Building
Prince Georges Center
Hyattsville, MD 20782
Attn: SEC 6034B
SEC 6110
SEC 6114H
SEC 6120
SEC 6136
SEC 6144G
SEC 6140B
SEC 6148

1 Naval Ship Engineering Center
Norfolk Division
Small Craft Engr Dept.
Norfolk, VA 23511
Attn: D. Blount (6660.03)

1 Library (Code 1640)
Naval Oceanographic Office
Washington, DC 20390

1 Commander (ADL)
Naval Air Development Center
Warminster, PA 18974

1 Naval Underwater Weapons Research
& Engineering Station (Library)
Newport, RI 02840

1 Commanding Officer (L31)
Naval Civil Engineering Laboratory
Port Hueneme, CA 93043

4 Commander
Naval Undersea Center
San Diego, CA 92132
Attn: Dr. A. Fabula (6005)
Dr. J. Hoyt (2501)
Library (13111)

1 Library
Naval Underwater Systems Center
Newport, RI 02840

1 Research Center Library
Waterways Experiment Station
Corp of Engineers
P.O. Box 631
Vicksburg, MS 39180

1 Dept. of Transportation
Library TAD-491.1
400 - 7th Street S.W.
Washington, DC 20590

1 Charleston Naval Shipyard
Technical Library
Naval Base
Charleston, SC 29408

1 Norfolk Naval Shipyard
Technical Library
Portsmouth, VA 23709

1 Philadelphia Naval Shipyard
Philadelphia, PA 19112
Attn: Code 240

1 Portsmouth Naval Shipyard
Technical Library
Portsmouth, NH 03801

1 Puget Sound Naval Shipyard
Engineering Library
Bremerton, WA 98314

1 Long Beach Naval Shipyard
Technical Library (246L)
Long Beach, CA 90801

1 Hunters Point Naval Shipyard
Technical Library (Code 202.3)
San Francisco, CA 94135

1 Pearl Harbor Naval Shipyard
Code 202.32
Box 400, FPO
San Francisco, CA 96610

1 Mare Island Naval Shipyard
Shipyard Technical Library
Code 202.3
Vallejo, CA 94592

1 Assistant Chief Design Engineer
for Naval Architecture (Code 250)
Mare Island Naval Shipyard
Vallejo, CA 94592

3 U.S. Naval Academy
Annapolis, MD 21402
Attn: Technical Library
Dr. Bruce Johnson
Prof. P. Van Mater, Jr.

1 Naval Postgraduate School
Monterey, CA 93940
Attn: Library, Code 2124

1 Capt. L.S. McCready, USMS
Director, National Maritime
Research Center
U.S. Merchant Marine Academy
Kings Point, L.I., NY 11204

1 U.S. Merchant Marine Academy
Kings Point, L.I., NY 11204
Attn: Academy Library

1 Bolt, Beranek & Newman
50 Moulton Street
Cambridge, MA 02138
Attn: Library

1 Bethlehem Steel Corporation
Center Technical Division
Sparrows Point Yard
Sparrows Point, MD 21219

1 Bethlehem Steel Corporation
25 Broadway
New York, NY 10004
Attn: Library (Shipbuilding)

1 Esso International
Design Division, Tanker Dept.
15 West 51st Street
New York, NY 10019

1 Mr. V. Boatwright, Jr.
R & D Manager
Electric Boat Division
General Dynamics Corporation
Groton, CT 06340

1 Gibbs & Cox, Inc.
21 West Street
New York, NY 10006
Attn: Technical Info. Control

1 Hydronautics, Inc.
Pindell School Road
Howard County
Laurel, MD 20810
Attn: Library

1 McDonnell Douglas Aircraft Co.
3855 Lakewood Blvd.
Long Beach, CA 90801
Attn: T. Cebeci

1 Lockheed Missiles & Space Co.
P.O. Box 504
Sunnyvale, CA 94088
Attn: Mr. R.L. Waid, Dept 57-74
Bldg. 150, Facility 1

1 Newport News Shipbuilding &
Dry Dock Company
4101 Washington Avenue
Newport News, VA 23607
Attn: Technical Library Dept.

1 Nielsen Engineering & Research Inc.
510 Clude Avenue
Mountain View, CA 94043
Attn: Mr. S. Spangler

1 Oceanics, Inc.
Technical Industrial Park
Plainview, L.I., NY 11803

1 Society of Naval Architects
and Marine Engineers
74 Trinity Place
New York, NY 10006
Attn: Technical Library

1 Sun Shipbuilding & Dry Dock Co.
Chester, PA 19000
Attn: Chief Naval Architect

1 Sperry Systems Management
Division
Sperry Rand Corporation
Great Neck, NY 11020
Attn: Technical Library

1 Stanford Research Institute
Menlo Park, CA 94025
Attn: Library G-021

2 Southwest Research Institute
P.O. Drawer 28510
San Antonio, TX 78284
Attn: Applied Mechanics Review
Dr. H. Abramson

1 Tracor, Inc.
6500 Tracor Lane
Austin, TX 78721

1 Mr. Robert Taggart
3930 Walnut Street
Fairfax, VA 22030

1 Ocean Engr. Department
Woods Hole Oceanographic Inst.
Woods Hole, MA 02543

1 Worcester Polytechnic Inst.
Alden Research Laboratories
Worcester, MA 01609

1 Applied Physics Laboratory
University of Washington
1013 N.E. 40th Street
Seattle, WA 98105
Attn: Technical Library

1 University of Bridgeport
Bridgeport, CT 06602
Attn: Dr. E. Uram

4 University of California
Naval Architecture Department
College of Engineering
Berkeley, CA 94720
Attn: Library
Prof. W. Webster
Prof. J. Paulling
Prof. J. Wehausen

3 California Institute of Technology
Pasadena, CA 91109
Attn: Aeronautics Library
Dr. T.Y. Wu
Dr. A.J. Acosta

1 Docs/Repts/Trans Section
Scripps Institution of
Oceanography Library
University of California,
San Diego
P.O. Box 2367
La Jolla, CA 92037

1 Catholic University of America
Washington, DC 20017
Attn: Dr. S. Heller, Dept of
Civil & Mech Engr

2 Florida Atlantic University
Ocean Engineering Department
Boca Raton, FL 33432
Attn: Technical Library
Dr. S. Dunne

1 University of Hawaii
Dept. of Ocean Engineering
2565 The Mall
Honolulu, HI 96822
Attn: Dr. C. Bretschneider

1 Institute of Hydraulic Research
The University of Iowa
Iowa City, IA 52240
Attn: Library

4 Department of Ocean Engineering
Massachusetts Insti. of Technology
Cambridge, MA 02139
Attn: Department Library
Prof. P. Mandel
Prof. M. Abkowitz
Dr. J. Newman

2 St. Anthony Falls Hydraulic Laboratory
University of Minnesota
Mississippi River at 3rd Ave. S.E.
Minneapolis, MN 55414
Attn: Prof. E. Silberman
Dr. C. Song

3 Department of Naval Architecture and Marine Engineering
University of Michigan
Ann Arbor, MI 48104
Attn: Library
Dr. T.F. Ogilvie
Prof. F. Hammitt

1 College of Engineering
University of Notre Dame
Notre Dame, IN 46555
Attn: Engineering Library

3 Davidson Laboratory
Stevens Institute of Technology
711 Hudson Street
Hoboken, NJ 07030
Attn: Library
Dr. J. Breslin
Dr. S. Tsakonas

2 Stanford University
Stanford, CA 94305
Attn: Engineering Library
Dr. R. Street

3 Webb Institute of Naval Architecture
Crescent Beach Road
Glen Cove, L.I., NY 11542
Attn: Library
Prof. E.V. Lewis
Prof. L.W. Ward

1 Applied Research Laboratory
P.O. Box 30
State College, PA 16801
Attn: Dr. B. Parkin, Director
Garfield Thomas
Water Tunnel

1 Dr. Michael E. McCormick
Naval Systems Engineering Dept.
U.S. Naval Academy
Annapolis, MD 21402

1 Dr. Douglas E. Humphreys (Code 712)
Naval Coastal Systems Laboratory
Panama City, FL 32401